University of Glasgow | School of Engineering

A New Digital PID Controller and Its Applications on DC-DC Converters

Chao Ding

Master of Philosophy

School of Engineering

University of Glasgow, Glasgow, United Kingdom

February 2020

Abstract

PID controller is widely employed in industry due to its simplicity and precise control. Lots of PID controllers are based on the pole placement method. However, the pole placement method is complicated for designers. Thus, in this report, a new digital PID controller is proposed to provide a simple PID controller with satisfactory performance. The proportional term is designed to guarantee the stability of the original proportional control system (without integral term and derivative term). The integral term is the same as conventional integral term to achieve zero steady-state error tracking. The conventional derivative term is replaced by a lead-phase compensator and it is connected with integrator in series. Comparing with conventional PID controllers, the number of control gains are reduced from three to two, which is easier to be designed. In addition, a tuning method for the new digital PID controller is proposed to adjust the error convergence rate. A numerical simulation example is implemented to test the performance of the new digital PID controller, and it is compared with conventional pole placement method. Finally, the new digital PID controller is employed on the DC-DC converters. The simulation results are analysed, and the results obtained show that the new digital PID controller has desired and satisfactory performance for DC-DC converters.

Table of Contents

List of Tables

List of Figures

List of Symbols

$A(z)$	denotes the denominator of $H(z)$
$B(z)$	denotes the numerator of $H(z)$
$B^{+}(z)$	denotes the cancellable portion of $B(z)$
$B^{-}(z)$	denotes the un-cancellable portion of $B(z)$
$B^{-*}(z)$	denotes the redesigned $B^{-}(z)$ by using ZMETC method
C	denotes the capacitor
d	denotes duty-cycle
$\hat{d}(t)$	denotes small signal perturbation of duty-cycle
D	denotes the steady-state value of duty-cycle
D'	denotes 1-D
$d(s)$	denotes disturbance
$e(z)$	denotes tracking error between input and output
$e_0(z)$	denotes tracking error which is produced by proportional control system
$G_m(s)$	denotes the transfer function of PID control system
$G_p(s)$	denotes the transfer function of plant
$G_L(s)$	denotes the transfer function of PID controller
$G_h(s)$	denotes the transfer function of Zero Order Hold
$G_{vd}(s)$	denotes the transfer function between output voltage and duty-cycle
$G_{buck}(s)$	denotes the transfer function between output and duty-cycle of Buck converter
$G_{boost}(s)$	denotes the transfer function between output and duty-cycle of Boost converter
$G_{buck-boost}(s)$	denotes the transfer function between output and duty-cycle of Buck-Boost converter
$G_I(z)$	denotes the transfer function of discrete redesigned integral term
$G_f(z)$	denotes the transfer function of discrete lead-phase compensator

$H(z)$	denotes the transfer function of designed control system
$\tilde{H(z)}^{-1}$	denotes the approximate inverse model
i_L	denotes the inductor current
$\hat{i}_L$	denotes the small signal perturbation of inductor current
I_L	denotes the steady-state value of inductor current
K_p	denotes the proportional gain
K_d	denotes the derivative gain
K_i	denotes the integral gain
K_I	denotes the gain of redesigned integral term
L	denotes the inductor
R	denotes the load
$r(s)$	denotes the reference signal
$r(t)$	denotes the step signal
$S_1(z)$	denotes the sensitive function of the PID control system
$S_0(z)$	denotes the sensitive function of proportional control system
$1/s$	denotes the Laplace transform of integrator
T_s	denotes the sampling time
T_{sf}	denotes the working period of switch
t_{on}	denotes the time period of "on" state of switch
v_{in}	denotes the voltage of power supply of converter
$\hat{v}_{in}$	denotes the small signal perturbation of input voltage of converter
V_{in}	denotes the steady-state value of input voltage of converter
v_{out}	denotes the output voltage of converter
$\hat{v}_{out}$	denotes the small signal perturbation of output voltage of converter
V_{out}	denotes the steady-state value of output voltage of converter
x	denotes the matrix composed by inductor current and output voltage
$y(s)$	denotes the output signal

ξ denotes the damping ratio

ω_n denotes the angular frequency

Declaration

“I declare that, except where explicit reference is made to the contribution of others, that this dissertation is the result of my own work and has not been submitted for any other degree at the University of Glasgow or any other institution.”

Printed Name: Chao Ding

Signature:

Acknowledgement

I would like to express my very great appreciation to my supervisor Keliang Zhou for his valuable and constructive suggestions and help during the planning and development of this research work. His willingness to give his time so generously has been very much appreciated.

I would like to offer my special thanks to my family for the unrequited support of my study and decisions. I also wish to thank my friends and girlfriend for the encourage they gave to me when I was confused and helpless.

1.Introduction

1.1. DC-DC Converters

The converters are power electronic circuit or electromechanical device which convert one level of electrical voltage to the desired voltage level [1]. The dc-dc converters are popular due to its high efficiency and small size. They are widely employed in switch-mode power supplies and dc motor drive applications [2]. There are mainly five kinds of dc-dc converters, Step-down (buck) converter, Step-up (boost) converter, Step-down/step-up (buck-boost) converter, Cuk converter and Full-bridge converter. The buck and boost converters are basic converter. Buck-boost converter and Cuk converter are composed by two topologies. The full-bridge converter is derived from buck converter [3].

The control strategies are important to the DC-DC converters which are employed to guarantee the output and performance of converters. There are many control strategies are used on converters such as Sliding mode control, Fuzzy logic control and PID control [3]. The Sliding Mode (SM) control designs a sliding surface in state space, and a control law is found to lead the trajectory of the system state to the sliding surface. In the end the system will reach the equilibrium point [1]. The SM control is easy to be implemented and the robustness is satisfactory. However, the converters which are controlled by SM are suffered from switching frequency variation [1]. The Fuzzy Logic (FL) control is popular in non-linear system, the first step is convert the input into a fuzzy set by using fuzzy linguistic, linguistic variables and membership functions. Then the fuzzy set is dealed by the fuzzy rule base and finally defuzzied by the defuzzier to create the control signals [3]. The FL control provides great robustness while the system is facing the time varying load, and it is suitable for the non-linear and model unknown models. However, the rule base of the FL control is based on the human experience, which is not reliable. The PID control strategy is widely employed on DC-DC converters. The proportional part provides a general control based on the error, the integral part guarantees the zero error tracking, and the derivative part improves the robustness. The PID control is easy to be implemented and the tracking performance is satisfactory. In this report, a new digital PID control method is proposed and simulated on DC-DC converters.

In this report, the Buck, Boost and Buck-Boost converter will be modelled, and the new digital PID controller will be employed to control the three kinds of converters above. The topologies of the three kinds of converters are shown in Figure 1-1.

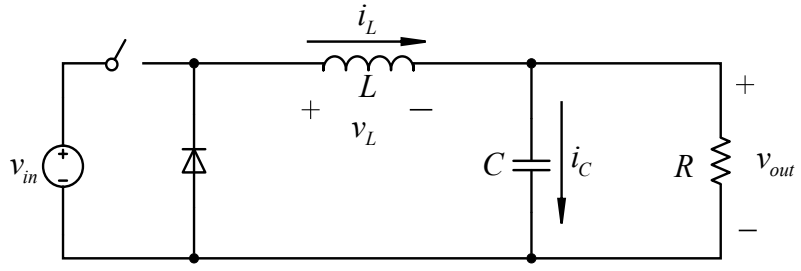

(a)

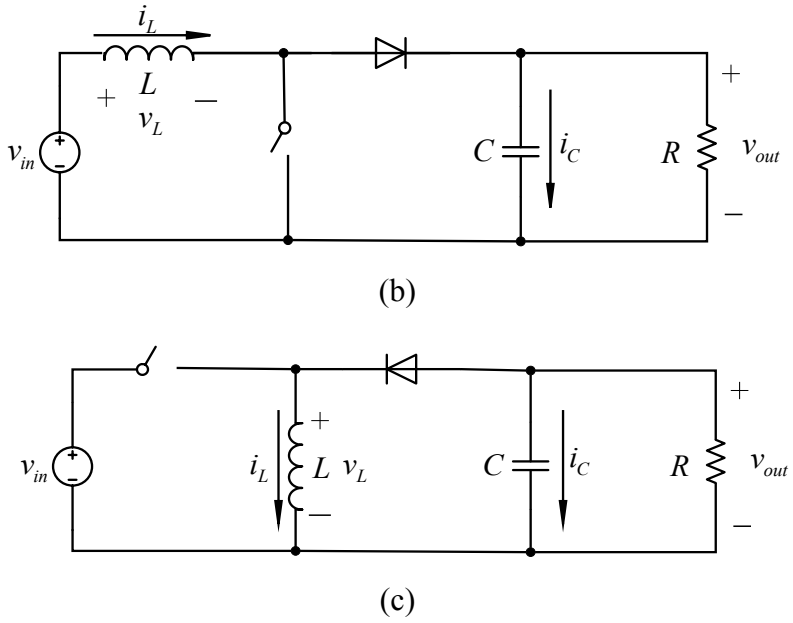

Fig. 1-1. The Topologies of Buck, Boost and Buck-Boost Converters. (a) Buck Converter, (b) Boost Converter, (c) Buck-Boost Converter.

The output voltages of DC-DC converters are required to be regulated, which means the outputs are required to be fixed and stable [4]. The unregulated or undesired output voltages will lead to unsatisfactory performance of converters. It is necessary to employ controllers to enhance the efficiency and performance of converters. The error signal is produced by comparing the output voltage with reference voltage, then the error signal is sent into the controller to provide control signal, which is used to change the state of the switch. Eventually the output voltage will track the reference voltage without any variation.

PID controllers are commonly employed in dc-dc converters due to its simple implementation and it is reliable for linear systems. The pole placement method is widely used to design PID controller. However, it is complicated especially for the high order system.

1.2. PID Control

PID controller is by far the most widely used controller today [5]. The PID control system is shown in Figure 1-2.

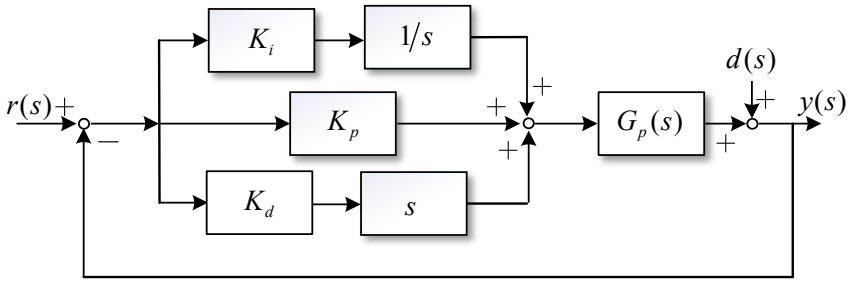

Fig. 1-2. The Structure of PID Control System

where $r(s)$, $y(s)$ and $d(s)$ are the reference input, output and disturbance respectively, $G_p(s)$ denotes the plant.

It is divided into three terms, Proportional (P), Integral (I) and Derivative (D) term, which are based on the present, past and future error respectively [5]. The proportional term is proportional to the current value of error and it provides a general control action [6]. However, using proportional term alone will lead to a steady-state error between the output signal and setpoint. To eliminate the steady-state error, the integral term is employed. The integral term integrates the past values of error over time to produce control signal. If the error exists, the integral term will keep working due to the historic cumulative value of error. The integral term will cease to grow if the error is eliminated. So that the integral term ensures the zero steady-state error tracking or eliminating of DC signal [7]. The integral term brings large delay to the system due to the integrations. To offset the delay, the derivative term is employed because of the 90-degree phase leading. In addition, the derivative term estimates the future trend of the error by calculating the rate of error change. It is so called the "anticipatory control". The derivative term will reduce the control effect if the error changes smooth. The control effect will be greater is the error changes rapidly.

The PID control is invented in 1910, numerous of design methods of PID controller are proposed during the last ten decades. The Ziegler-Nichols [8] and Cohen-Coon [9] methods are two basic methods which are based on the experience in manual tuning. These two methods are mainly employed for the process which has large time delays such as chemical process. In addition, these two methods provide unsatisfactory damping ratio [10] and the stability criterions are not clearly described. Except the Z-N and C-C methods, some model based PID design methods are proposed. Such as pole placement method [11], dominant pole placement method [12, 13], Haalman method [11, 14], gain and phase

margin-based design methods [15-17]. The pole placement method allows the designers to place the poles of the closed-loop system in desired locations by adding a controller, so that the dynamics of the system is desired. However, the arbitrary pole placement is difficult to achieve if the plant is high-order and the controller is low-order. To overcome this problem, the dominant pole placement is proposed [12, 18]. The idea behind the dominant pole placement method is putting two closed-loop poles into dominant region, and the other poles are outside the region [12]. A conventional dominant pole placement method is proposed [19]. It is based on the simplified model of plants. However, the dominance of the chosen poles cannot be guaranteed. In addition, this method will lead to instability of the closed-loop system if not well handled. In the light of above, the pole placement method is complicated or even unavailable for the high-order system. Haalman method can be considered as pole-zero cancel method. It provides a controller which is able to cancel the poles and zeros of the process to achieve desired performance and dynamics. The drawback of Haalman method is that all the poles and zeros of the process are cancelled, which may cause the losing of controllability of controller, which means the controller will not able to reduce the error [5]. It is known from classical control that the phase margin is related to the damping of the system, the gain margin and phase margin can be considered as a performance measure. The gain and phase margin-based method provides a controller to satisfy the gain margin and phase margin criteria of a closed-loop system [17]. However, it is complicated to express the gain and phase margins of the system. In the light of above, the stability criterion and tuning method for conventional PID controller are associated to three control gains, which are complicated and hard to obtain.

In this report, a new digital PID controller is proposed. The topology is equivalent as conventional PID controller. However, comparing with conventional PID controller, it is much easier to be designed. The derivative term of this new digital PID controller is replaced by a lead-phase compensator, which is able to provide leading phase. It is connected to the integral term in series instead of paralleling. Such a lead-phase compensator can be considered as a general derivative term. The lead-phase compensator is based on the pole-zero cancellation method. It simplifies the derivation of stability criterions. The stability criterions of the system with new designed PID controller is derived. In addition, a tuning method is proposed to provide the guide to adjust the error convergence rate. Finally, some simulations are implemented to show the performance of the new digital PID controller.

1.3. Organization of Report

The rest of this report is organized as follows: Section 2 is the design method of new digital PID controller. Section 3 shows the design process of the new design digital PID controller, including the structure, the stability criterion and a tuning method. Section 4 shows the modelling of converters and some simulations. Section 5 is the conclusion.

2. New Digital PID Controller

2.1 Introduction

In this chapter, the new digital PID controller is introduced, including the structure, the derivation of stability criterion and the tuning method for error convergence rate. The number of control gains of the new digital PID controller is reduced from three to two. So that the complexity of design can be reduced. In addition, a numerical model simulation will be implemented to test the performance of the new digital PID controller.

2.2 The Topology of the New Digital PID Controller

The Laplace transform of the conventional PID controller is expressed as:

$$G_L(s) = K_p + K_i \frac{1}{s} + K_d s \tag{2.1}$$

where K_p , K_i and K_d represent the proportional, integral and derivative gains respectively, $1/s$ denotes the integrator and s is the differentiator. The structure of conventional PID control system is shown in Figure. 1-2. The expression of conventional PID controller can be equivalent as:

$$G_L(s) = K_p + K_I \frac{1}{s}\left(\frac{K_i + K_d s^2}{K_I}\right) \tag{2.2}$$

where $G_f(s) = (K_i + K_d s^2)/K_I$. The $G_f(s)$ is a lead-phase compensator which is employed to provide lead phase to compensate the phase delay of the system.

The conventional derivative term provides 90-degree leading phase to offset the phase delay produced by integrator. The damping ratio and robustness of the system can be improved. The conventional derivative term can be considered as a lead-phase compensator which provides 90-degree leading phase to improve the robustness and transient dynamics, so that a lead-phase compensator which is able to provide leading phase can be considered as a general derivative term.

The structure of the equivalent PID control system is shown in Figure. 2-1. In the new digital PID controller, the lead-phase compensator $G_f(s)$ is based on pole-zero cancellation method, and it is related to the process. The conventional derivative term is replaced by the lead-phase compensator, and it is combined with integrator in series to form a new integral term $G_I(s)$. K_I denotes the control gain of the new integral term.

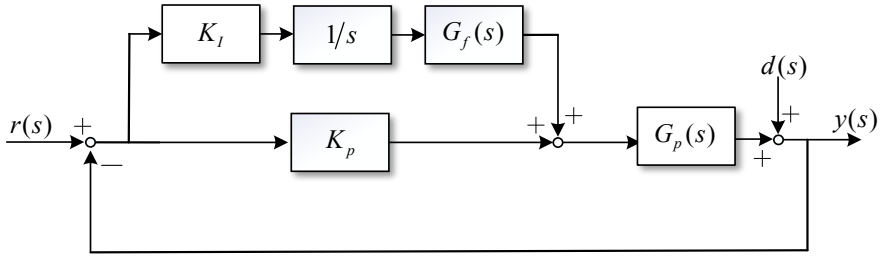

Fig. 2-1. The Structure of Equivalent PID Control System

Comparing with conventional PID control system, the equivalent PID control system is easier to be designed. For conventional PID control system, the three control parameters (K_p, K_i and K_d) makes the design complicated. However, the number of control elements is reduced from three to two (K_p and K_I) for the new digital PID controller if the lead-phase compensator is fixed. The complexity of designing is eased.

With advances in digital technology, PID control systems are usually implemented in the digital form. Euler method is a feasible method which is used to transfer the differential equation of continues time domain to difference equation of discrete time domain. The discrete integrator can be obtained as $T_s/(z-1)$ by using Forward Euler method. The equivalent PID control system is transferred into digital form which is shown in Figure. 2-2.

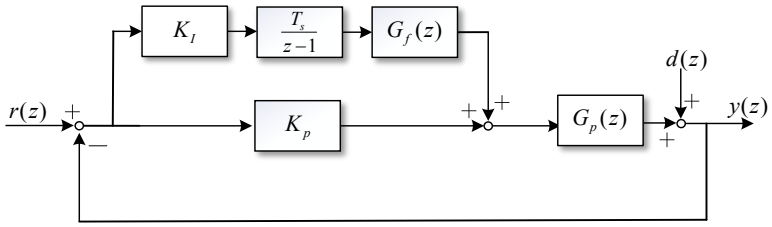

Fig. 2-2. The Structure of New Digital PID Control System

2.3 Stability Criterion and The Lead-Phase Compensator

The new integral term is composed by a conventional digital integrator, the integral gain and a lead-phase compensator. The expression of the new integral term is:

$$G_I(z) = K_I \frac{T_s}{z-1} G_f(z) \tag{2.3}$$

K_I denotes the control gain of the new integral term, $G_f(z)$ is the lead-phase compensator which is employed to replace the derivative term and provide leading phase. According to Fig. 2-2, the output of the digital PID control system is:

$$y(z) = \frac{[K_p + G_I(z)]H(z)}{1 + G_I(z)H(z)} r(z) + \frac{[1 + K_p G_p(z)]^{-1}}{1 + G_I(z)H(z)} d(z) \text{ [20]} \tag{2.4}$$

where $H(z)$ is designed as:

$$H(z) = \frac{G_p(z)}{1 + K_p G_p(z)} \tag{2.5}$$

$G_I(z)$ denotes the new digital integral term, $G_p(z)$ is the plant. From Eq. 2.4, the digital PID control system is stable if the following two conditions are satisfied [20]:

1. Roots of $1+K_pG_p(z)=0$ are inside the unit circle. The closed-loop feedback control system is stable without the plug-in new integral term.

2. Roots of $1+G_I(z)H(z)=0$ are inside the unit circle.

Based on Eq. 2.3, the roots of $1+G_I(z)H(z)=0$ is expressed as:

$$|z|=\left|1-K_IT_sG_f(z)H(z)\right| \tag{2.6}$$

According to the equation above, the condition 2 becomes:

$$\left|1-K_IT_sG_f(z)H(z)\right|\le 1 \tag{2.7}$$

It can be obtained that Eq. 2.7 can be simplified if the lead-phase compensator is the inverse of $H(z)$ i.e., $G_f(z)=1/H(z)$ and $H(z)$ can be expressed in a general way as:

$$H(z)=\frac{G_p(z)}{1+K_pG_p(z)}=\frac{B(z)}{A(z)}=\frac{z^{-d}B^+(z)B^-(z)}{A(z)} \text{ [20]} \tag{2.8}$$

where d denotes the pure time delay steps which is normally caused by the delay plant. The roots of $A(z)=0$ are inside the unit circle, $B^+(z)$ and $B^-(z)$ are, respective, the cancellable and un-cancellable portions of $B(z)$. In addition, $B^-(z)$ contains the roots on or outside the unit circle and undesired roots, $B^+(z)$ contains the other roots of $B(z)$ [21-25]. The lead-phase compensator $G_f(z)$ can designed based on pole-zero cancellation method which is shown as:

$$G_f(z) = \frac{z^d A(z) B^-(z^{-1})}{B^+(z) b} \text{ [20]} \tag{2.9}$$

where z^d denotes a d step lead. Since $B^-(z)$ contains the roots which are outside the unit circle, $B^-(z)$ is transferred as $B^-(z^{-1})$ with z replaced by z^{-1} so that $G_f(z)$ is stable, b is employed to scale the steady state gain of $G_f(z)$, and $b \geq \max \left| B^-(1) \right|^2$. Based on above, we have:

$$g = \left| G_f(z) H(z) \right| = \frac{B^-(z) B^-(z^{-1})}{b} \leq 1 \text{ [20]} \tag{2.10}$$

Based on Eq. 2.7-2.10, the condition 2 can be simplified as:

$$0 < K_I < \frac{2}{T_s} \tag{2.11}$$

In the light of above, the stability criterion of the new design method is associated with two parameters i.e. K_p and K_I. K_I has a certain range which means if the original proportional control system is stable, the new design method based system is guaranteed stable if the new integral gain is selected form the range. Comparing with conventional PID control system, the complexity is reduced significantly. For conventional design method of PID control system, the stability criterion is related to three parameters, which is more complicated than this new design method.

2.4 Tuning Method for Error Convergence Rate

When the plug-in integral term is absent, the tracking error of the closed-loop control system can be expressed as:

$$e(z)=\frac{r(z)-d(z)}{[1+G_I(z)H(z)][1+K_pG_p(z)]}=\frac{e_0(z)}{1+G_I(z)H(z)} \tag{2.12}$$

where $S_1(z)=(1+G_I(z)H(z))^{-1}$ and $S_0(z)=(1+K_pG_p(z))^{-1}$ are the sensitive functions which are used to define the error attenuations of the plug-in integral term $G_I(z)$ and Proportional controller K_p respectively. $e_0(z)$ represents the tracking error which is produced by the Proportional control system without the plug-in integral term. It is easy to figure out that the error attenuation is inversely proportional to $|S_1(z)|$ or $|S_0(z)|$. Assuming that the proportional control system is stable without the plug-in integral term, which means the error $e_0(z)$ is a steady signal, so that the $|S_0(z)|$ can be considered as a constant value. Therefore, the error attenuation of the digital PID control system is controlled by $|S_1(z)|$, which means the error convergence rate is controlled by the plug-in integral term. The sensitivity function $S_1(z)$ is:

$$S_1(z)=\frac{1-z^{-1}}{1-(1-K_IT_sg)z^{-1}}\ [20] \tag{2.13}$$

Using inverse z-transform, we have:

$$S_1(n)=-K_IT_sg(1-K_IT_sg)^{n-1},n\geq 0\ [20] \tag{2.14}$$

The stability criterion which is described by Eq. 2.11 leads to $-1<1-K_IT_sg<1$. If n is infinity, $(1-K_IT_sg)^{n-1}$ will become 0, which leads the sensitivity function $S_1(n)$ to 0, i.e., the plug-in integral term can eliminate the error to zero. More importantly, it can be obtained that the error convergence rate of the digital PID controller is determined by the plug-in integral gain K_I, i.e., larger K_I leads to faster convergence rate while smaller K_I leads to slower convergence rate.

2.5. The Numerical Model Simulation

The reference signal is a step signal, $r(t) = 1$ for $t \geq 0$ s and the plant is a typical first order system which is shown as below:

$$G_p(s) = \frac{1}{s+1} \tag{2.15}$$

2.5.1 The Pole Placement PID Controller Design Method

In this section, a conventional PID controller is designed based on the pole placement method. The transfer function of a conventional PID control system is:

$$G_m(s) = \frac{G_L(s)G_p(s)}{1+G_L(s)G_p(s)} \tag{2.16}$$

Where $G_L(s)$ represents conventional PID controller, substitute the expression of $G_p(s)$ into the equation above, we have:

$$G_m(s) = \frac{\frac{K_d}{1+K_d}s^2 + \frac{K_p}{1+K_d}s + \frac{K_i}{1+K_d}}{s^2 + \frac{1+K_p}{1+K_d}s + \frac{K_i}{1+K_d}} \tag{2.17}$$

The characteristic equation of $G_m(s)$ is:

$$s^2 + \frac{1+K_p}{1+K_d}s + \frac{K_i}{1+K_d} = 0 \tag{2.18}$$

The characteristic equation can be compared with the typical second order model, which is:

$$s^2 + 2\xi\omega_n s + \omega_n{}^2 = 0 \tag{2.19}$$

where ξ and ω_n ($\omega_n > 0 rad/s$) represent the damping ratio and natural frequency of the system respectively. According to the two equations above, the expressions of damping ratio and natural frequency can be obtained as:

$$\begin{aligned} \omega_n &= \sqrt{\frac{K_i}{1+K_d}} \\ \xi &= \frac{1+K_p}{2\omega_n(1+K_d)} = \frac{1+K_p}{2\sqrt{K_i(1+K_d)}} \end{aligned} \tag{2.20}$$

Based on the equations above, a conventional PID controller can be designed with certain damping ratio and two of the three control gains. For example, the pole placement method based PID control system is designed with different damping ratio. The proportional gain and derivative gain are fixed as 0.5 and 0.01 respectively. The damping ratios are chosen as 0.6, 0.707, 1 and 1.2. The parameters are shown in Table 1.

Table 1. Parameters of Different Damping Ratio with Fixed K_p and K_d for First Order Plant

K_p	K_d	K_i	ξ	ω_n
0.5	0.01	1.55	0.6	1.4851
0.5	0.01	1.1142	0.707	1.0503
0.5	0.01	0.557	1	0.7426
0.5	0.01	0.387	1.2	0.62

The responses are shown in Figure 2-3.

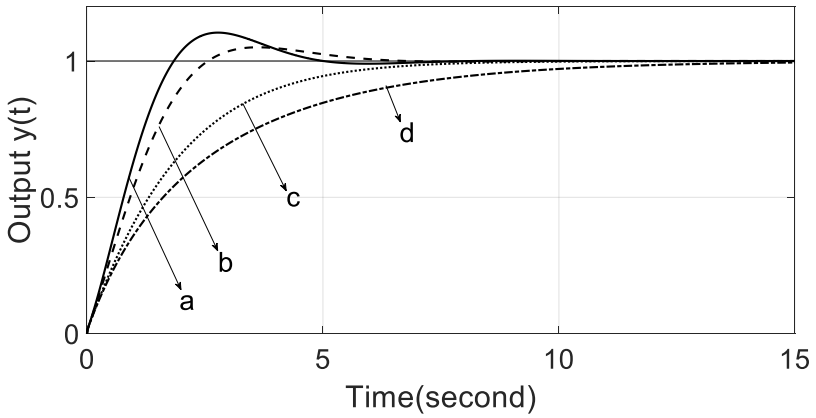

Fig. 2-3. The Responses for Different Damping Ratio with Fixed Proportional Gain with (a) Damping ratio 0.6, $K_i = 1.55$, (b) Damping ratio 0.707, $K_i = 1.1142$, (c) Damping ratio 1, $K_i = 0.557$, (c) Damping ratio 1.2, $K_i = 0.387$

2.5.2 The New Digital PID Controller Design Method

The plant can be transferred from continues time domain into discrete time domain by using Zero Order Hold (ZOH) method. The Laplace transform transfer function of the Zero Order Hold is:

$$G_h(s) = \frac{1 - e^{-sT_s}}{s} \tag{2.21}$$

$H(s)$ is:

$$H(s) = \frac{G_p(s)}{1 + K_p G_p(s)} = \frac{1}{s + 1 + K_p} \tag{2.22}$$

After adding a zero-order hold, we have:

$$G_{hp}(s) = G_h(s)H(s) = \frac{1 - e^{-sT_s}}{s(s + 1 + K_p)} \tag{2.23}$$

The discrete plant can be obtained by using Z-transform on the plant and the sampling time is 0.0001s, so that $H(z)$ is:

$$H(z) = \frac{G_p(z)}{1 + K_p G_p(z)} = \frac{0.0009995}{z - 0.999 + 0.0009995K_p} \tag{2.24}$$

The lead-phase compensator $G_f(z)$ can be written as:

$$G_f(z) = \frac{1}{H(z)} = \frac{z - 0.999 + 0.0009995K_p}{0.0009995} \tag{2.25}$$

The new integral term is composed by the combination of lead-phase compensator and discrete integrator. The new integral term is expressed as:

$$G_I(z) = K_I \frac{T_s}{z - 1} G_f(z) = \frac{K_I T_s z - K_I T_s (0.0009995K_p - 0.999)}{0.0009995z - 0.0009995} \tag{2.26}$$

2.5.3 Simulations and Results

In this section, the simulations will be implemented in two ways. A. The numerical model simulation with the absence of lead-phase compensator. B. Comparison between conventional PID controller which is designed by pole placement method and new digital PID controller. In addition, the simulation results will be analysed.

a. Without Lead-phase Compensator

In this case, the proportional gain K_p is chosen as 0.5. According to condition 2, the roots of $1+G_I(z)H(z)=0$ without lead-phase compensator becomes:

$$|z|=\left|\frac{1.9980005\pm\sqrt{1.9980005^2-4(0.0009995K_IT_s+0.9980005)}}{2}\right|$$

Condition 2 becomes:

$$0<K_I<\frac{1.0005}{T_s}$$

It can be obtained that the stability criterion for K_I becomes narrower without the lead-phase compensator. The new integral gain for the digital PID control system without lead-phase compensator is chosen as 1. The parameters are shown in Table. 2.

Table 2. Parameters of New Design Method for First Order Plant with and without $G_f(z)$

	K_I	K_p	$G_I(z)$
With $G_f(z)$	1	0.5	$\frac{0.001z-0.00099850025}{0.0009995z-0.0009995}$
Without $G_f(z)$	1	0.5	$\frac{T_s}{z-1}$

The responses for the digital PID control systems with and without lead-phase compensator are shown in Figure. 2-4.

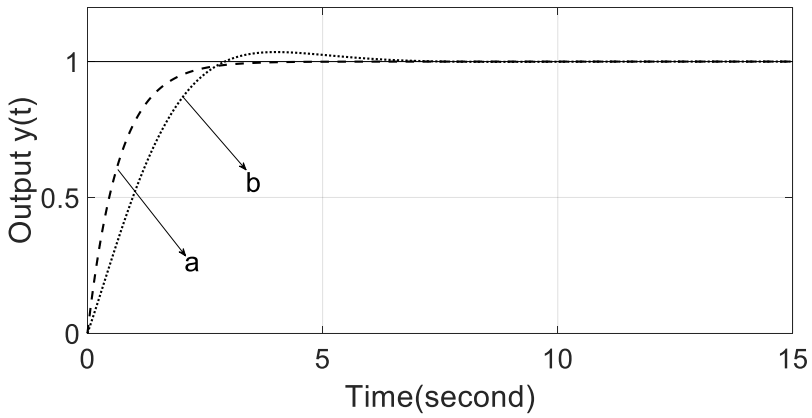

Fig. 2-4. The Responses for Digital PID Control System with and without Lead-phase Compensator. (a) With Lead-phase Compensator, (b) Without Lead-phase Compensator.

From Figure. 2-4, it can be obtained that the lead-phase compensator is able to suppress the overshoot, which means the lead-phase compensator enhances the damping ratio of the entire system, which is same as derivative term. In addition, the lead-phase compensator improves the response speed as well.

b. Comparing Between Pole Placement PID Controller and New Digital PID Controller

In this case, the new digital PID controller is compared with pole placement digital PID controller with different damping ratio and fixed proportional gain. The proportional gain and derivative gain are fixed as 0.5 and 0.01. The damping ratios are 0.6, 0.707, 1 and 1.2, the corresponding integral gains are 1.55, 1.1142, 0.557 and 0.387 respectively. The parameters are shown in Table 3 and the response are shown in Figure 2-5.

Table 3. Parameters of Two Kinds of PID Controllers for First Order Plant with Fixed K_p and K_d

Controllers	ξ	K_p	K_d	K_i
Pole Placement PID	0.6	0.5	0.01	1.55
Pole Placement PID	0.707	0.5	0.01	1.1142
Pole Placement PID	1	0.5	0.01	0.557
Pole Placement PID	1.2	0.5	0.01	0.387
New Digital PID	*	0.5	$G_f(z)$	1.55
New Digital PID	*	0.5	$G_f(z)$	1.1142
New Digital PID	*	0.5	$G_f(z)$	0.557
New Digital PID	*	0.5	$G_f(z)$	0.387

The responses are shown in Figure 2-5.

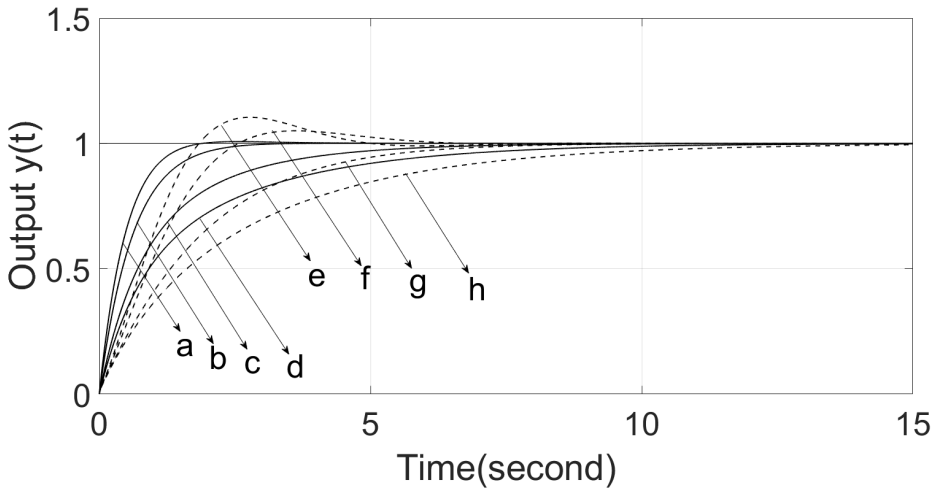

Fig.2-5. Comparison of Responses Between Two Kinds of PID Controllers with Fixed K_p and K_d. (a) to (d) are Responses for New Digital PID Controller with Ki=1.55, 1.1142, 0.557, and 0.387 Respectively. (e) to (h) are Responses for Pole Placement PID Controller with 0.6, 0.707, 1 and 1.2 Damping Ratios, Ki=1.55, 1.1142, 0.557 and 0.387 Respectively.

According to Figure. 2-5, the responses for the system with new digital PID controller have shorter rise time than the responses for pole placement method with the same value of integral gain. The overshoot is suppressed with new digital PID controller. In addition, comparing the system with pole placement PID controller, the error convergence rate of the responses is faster with new digital PID controller. The tuning method for error convergence rate is also verified by Figure 2-5, larger integral gain leads to faster error convergence rate. In the light of above, for a first order plant, the new digital PID controller has better control performance, especially the elimination of overshoot.

2.6 Summary

In this chapter, the new digital PID controller design method is introduced. It can be obtained that the stability criterion of the new method is easer than pole placement method. The stability criterion of the new method is associated with two control gains, the integral gain and the proportional gain. In addition, the integral gain has a certain range, which means the system is stable if the integral gain is chosen from such certain range.

According to the simulation results, for a simple first order plant, the new digital PID controller supresses the overshoot significantly. In addition, the error convergence rate is fast.

3. The New Digital PID Controller of DC-DC Converters

3.1 Introduction

In this chapter, the new digital PID controller is used on three kinds of DC-DC converters (BUCK, BOOST, BUCK-BOOST). The converters are modelled by small signal method. The performance of new digital PID controller for converters will be shown by some simulations. In addition, the new digital PID controller is compared with conventional PID controller which is based on pole placement method to demonstrate the advantages and disadvantages.

3.2 DC-DC Buck Converter

The buck converter converts low level voltage to high level voltage. It is normally employed in regulated dc power supplies and dc motor speed control [3]. When the switch is on, the diode is reverse biased, and the power source provides energy to load and inductor. During this time period, the inductor stores energy in the form of magnetic field. If the switch is opened while the current is still changing, a voltage drop will exist across the inductor. So that the output voltage (load voltage) will be less than input voltage. When the switch is off, the dc voltage source will be removed from the circuit. The inductor becomes a current source, which means the stored energy in inductor will provides current flow to load.

3.2.1 Small Signal Modeling of DC-DC Buck Converter

The circuit of a DC-DC Buck converter is shown is Figure 3-1.

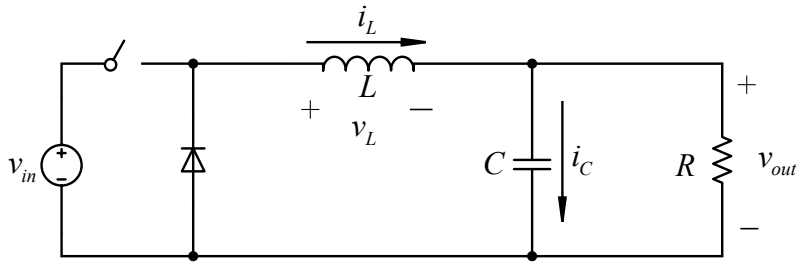

Figure. 3-1. The Circuit of Buck Converter

where v_{in} and v_{out} represent the input voltage and output voltage respectively, i_L denotes the inductor current, L, C and R represent the values of inductor, capacitor and load respectively.

When the switch is turned on, the buck converter is shown in Figure 3-2.

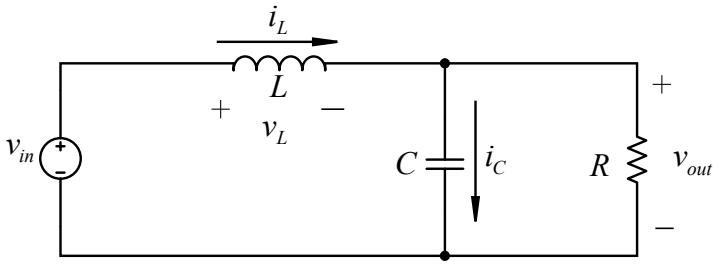

Figure. 3-2. The Circuit of Buck Converter When Switch is Turned On

The dynamics of DC-DC Buck Converter when the switch is turned on can be described as follow:

$$\begin{bmatrix} \frac{di_L(t)}{dt} \\ \frac{dv_{out}(t)}{dt} \end{bmatrix} = \begin{bmatrix} 0 & -\frac{1}{L} \\ \frac{1}{C} & -\frac{1}{RC} \end{bmatrix} \begin{bmatrix} i_L(t) \\ v_{out}(t) \end{bmatrix} + \begin{bmatrix} \frac{1}{L} \\ 0 \end{bmatrix} v_{in} \tag{3.1}$$

Let:

$$x=\begin{bmatrix} i_L(t) \\ v_{out}(t) \end{bmatrix}, A_1=\begin{bmatrix} 0 & -\frac{1}{L} \\ \frac{1}{C} & -\frac{1}{RC} \end{bmatrix}, B_1=\begin{bmatrix} \frac{1}{L} \\ 0 \end{bmatrix}, C_1=\begin{bmatrix} 0 \\ 1 \end{bmatrix} \tag{3.2}$$

So that we have the state space equation to describe the converter as:

$$\begin{cases} x = A_1 x + B_1 v_{in} \\ v_{out}(t) = C_1 x \end{cases} \tag{3.3}$$

When the switch is turned off, the diagram is shown in Figure 3-3.

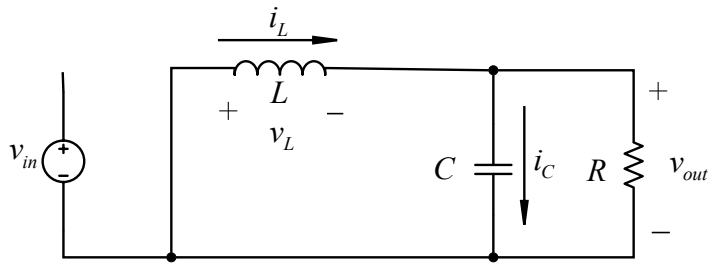

Figure. 3-3. The Circuit of Buck Converter When Switch is Turned Off

The dynamics of buck converter can be described as:

$$\begin{bmatrix} \frac{di_L(t)}{dt} \\ \frac{dv_{out}(t)}{dt} \end{bmatrix} = \begin{bmatrix} 0 & -\frac{1}{L} \\ \frac{1}{C} & -\frac{1}{RC} \end{bmatrix} \begin{bmatrix} i_L(t) \\ v_{out}(t) \end{bmatrix} + \begin{bmatrix} 0 \\ 0 \end{bmatrix} v_{in} \tag{3.4}$$

where

$$A_2 = \begin{bmatrix} 0 & -\frac{1}{L} \\ \frac{1}{C} & -\frac{1}{RC} \end{bmatrix}, B_2 = \begin{bmatrix} 0 \\ 0 \end{bmatrix}, C_2 = \begin{bmatrix} 0 \\ 1 \end{bmatrix} \tag{3.5}$$

The state space equation for the converter when the switch is turned off can be described as:

$$\begin{cases} x = A_2 x + B_2 v_{in} \\ v_{out}(t) = C_2 x \end{cases} \tag{3.6}$$

Based on the state space averaging technique, the average of the two states above can be expressed as follow:

$$\begin{cases} x = [A_1 d + A_2(1-d)]x + [B_1 d + B_2(1-d)]v_{in} \\ v_{out} = [C_1 d + C_2(1-d)]x \end{cases} \tag{3.7}$$

where d denotes the duty cycle which is defined as the ratio of the on duration to the switching time period. It can be expressed as:

$$d = \frac{t_{on}}{T_{sf}} \tag{3.8}$$

where t_{on} denotes switch on duration, and T_{sf} represents the switching period. The average state space function of the Buck converter is:

$$\begin{bmatrix} \frac{di_L(t)}{dt} \\ \frac{dv_{out}(t)}{dt} \end{bmatrix} = \begin{bmatrix} 0 & -\frac{1}{L} \\ \frac{1}{C} & -\frac{1}{RC} \end{bmatrix} \begin{bmatrix} i_L(t) \\ v_{out}(t) \end{bmatrix} + \begin{bmatrix} \frac{i_{in}}{L} \\ 0 \end{bmatrix} d \tag{3.9}$$

Thus, we have the inductor voltage and output current as:

$$\begin{cases} \frac{di_L(t)}{dt} = \frac{d}{L} v_{in} - \frac{1}{L} v_{out}(t) \\ \frac{dv_{out}(t)}{dt} = \frac{1}{C} i_L(t) - \frac{v_{out}(t)}{RC} \end{cases} \tag{3.10}$$

The state-space averaging over one switching period eliminates the switching ripples in inductor current and capacitor voltage. However, the nonlinearities are brought to the averaging model. The system is linearized by constructing a small-signal model. To construct a small-signal ac model at a quiescent operating point, we assume:

$$\begin{aligned} i_L(t) &= I_L + \hat{i}_L(t) \\ v_{in}(t) &= V_{in} + \hat{v}_{in}(t) \\ v_{out}(t) &= V_{out} + \hat{v}_{out}(t) \\ d(t) &= D + \hat{d}(t) \end{aligned} \tag{3.11}$$

where $\hat{i}_L$, $\hat{v}_{in}$, $\hat{v}_{out}$ and $\hat{d}(t)$ represent the small AC perturbations, I_L , V_{in} , V_{out} and D represent the steady-state values. Based on the equations above, the small signal model of buck converter is described as:

$$\begin{bmatrix} \dfrac{d(I_L+\hat{i}_L(t))}{dt} \\ \dfrac{d(V_{out}+\hat{v}_{out}(t))}{dt} \end{bmatrix} = \begin{bmatrix} 0 & -\dfrac{1}{L} \\ \dfrac{1}{C} & -\dfrac{1}{RC} \end{bmatrix} \begin{bmatrix} I_L+\hat{i}_L(t) \\ V_{out}+\hat{v}_{out}(t) \end{bmatrix} + \begin{bmatrix} \dfrac{V_{in}+\hat{v}_{in}(t)}{L} \\ 0 \end{bmatrix} (D+\hat{d}(t)) \tag{3.12}$$

$$\begin{cases} \dfrac{d(I_L+\hat{i}_L(t))}{dt} = \dfrac{D+\hat{d}(t)}{L}(V_{in}+\hat{v}_{in}(t)) - \dfrac{1}{L}(V_{out}+\hat{v}_{out}(t)) \\ \dfrac{d(V_{out}+\hat{v}_{out}(t))}{dt} = \dfrac{1}{C}(I_L+\hat{i}_L(t)) - \dfrac{V_{out}+\hat{v}_{out}(t)}{RC} \end{cases} \tag{3.13}$$

Omitting the high-order small signal terms and DC terms, we have:

$$\begin{cases} \dfrac{d\hat{i}_L(t)}{dt} = \dfrac{V_{in}}{L}\hat{d}(t) + \dfrac{D}{L}\hat{v}_{in}(t) - \dfrac{1}{L}\hat{v}_{out}(t) \\ \dfrac{d\hat{v}_{out}(t)}{dt} = \dfrac{1}{C}\hat{i}_L(t) - \dfrac{\hat{v}_{out}(t)}{R} \end{cases} \tag{3.14}$$

The small signal model of buck converter is shown in Figure 3-4.

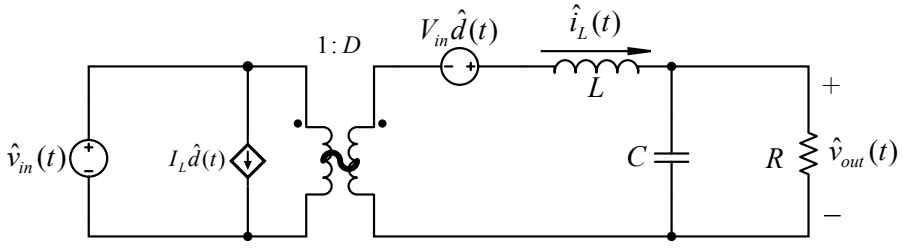

Figure. 3-4. The Small Signal Model of Buck Converter

Using Laplace transform, we have:

$$\begin{cases} si_L(s) = \dfrac{d(s)}{L}V_{in} + \dfrac{D}{L}v_{in}(s) - \dfrac{1}{L}v_{out}(s) \\ sv_{out}(s) = \dfrac{1}{C}i_L(s) - \dfrac{1}{RC}v_{out}(s) \end{cases} \tag{3.15}$$

In the light of above, the transfer function between duty cycle and output voltage can be expressed as:

$$G_{vd}(s) = \left.\frac{v_{out}(s)}{d(s)}\right|_{v_{in}(s)=0} = \frac{\dfrac{1}{CL}V_{in}}{s^2 + s\dfrac{1}{RC} + \dfrac{1}{CL}} = \frac{K_2K_3V_{in}}{s^2 + sK_4 + K_2K_3} \tag{3.16}$$

where:

$$K_1 = \frac{D}{L}, K_2 = \frac{1}{L}, K_3 = \frac{1}{C}, K_4 = \frac{1}{RC} \tag{3.17}$$

3.2.2 Conventional PID Controller Design of DC-DC Buck Converter

In this report, a conventional PID controller is designed based on the pole placement method. The transfer function of a conventional PID controller is:

$$G_L(s) = K_p + K_i\frac{1}{s} + K_d s \tag{3.18}$$

The transfer function of a conventional PID control system is:

$$G_m(s) = \frac{G_L(s)G_{vd}(s)}{1 + G_L(s)G_{vd}(s)} \tag{3.19}$$

The characteristic equation of $G_m(s)$ is:

$$s^3 + (K_4 + K_2K_3K_dV_{in})s^2 + (K_2K_3 + K_2K_3K_pV_{in})s + K_2K_3K_iV_{in} \tag{3.20}$$

A suitable closed-loop characteristic equation of a third order system can be written as:

$$(s + \alpha\omega_n)(s^2 + 2\xi\omega_n s + \omega_n{}^2) = 0 \tag{3.21}$$

where ξ and ω_n denote the damping ratio and natural frequency respectively. α is a constant. We have:

$$\begin{aligned} K_4 + K_2K_3K_dV_{in} &= \omega_n(\alpha + 2\xi) \\ K_2K_3 + K_2K_3K_pV_{in} &= \omega_n{}^2(1 + 2\xi\alpha) \\ K_2K_3K_iV_{in} &= \alpha\omega_n{}^3 \end{aligned} \tag{3.22}$$

The three control gains of PID controller can be expressed as:

$$\begin{aligned} K_p &= \frac{\omega_n{}^2(1 + 2\xi\alpha) - K_2K_3}{K_2K_3V_{in}} \\ K_d &= \frac{\omega_n(\alpha + 2\xi) - K_4}{K_2K_3V_{in}} \\ K_i &= \frac{\alpha\omega_n{}^3}{K_2K_3V_{in}} \end{aligned} \tag{3.23}$$

In this case, $L = 2mH, C = 20\mu F, R = 0.5\Omega, V_{in} = 40V, D = 0.5$. The proportional gain and derivative gain are fixed as 0.5 and 0.001 respectively. The values of ξ are 0.6, 0.707, 1 and 1.2 respectively. The parameters for Buck converter and PID controller are shown in Table 4 and Table 5 respectively.

Table 4. The parameters for Buck Converter

$L(H)$	2×10^{-3}
$C(F)$	2×10^{-5}
$R(\Omega)$	0.5
$V_{in}(V)$	40
$V_{out}(V)$	20
D	0.5

Table 5. Parameters of Conventional PID Controller for Buck Converter with Fixed K_p, K_d

K_p	K_d	K_i	ξ	$\omega_n(rad/s)$	α
0.5	0.001	174	0.6	397.78	2764.15
0.5	0.001	125.314	0.707	337.607	3256.812
0.5	0.001	62.6556	1	238.714	4606.023
0.5	0.001	43.5138	1.2	198.935	5527.04

The responses are shown in Figure 3-5. The Y-axis Output y(t) denotes the output voltage.

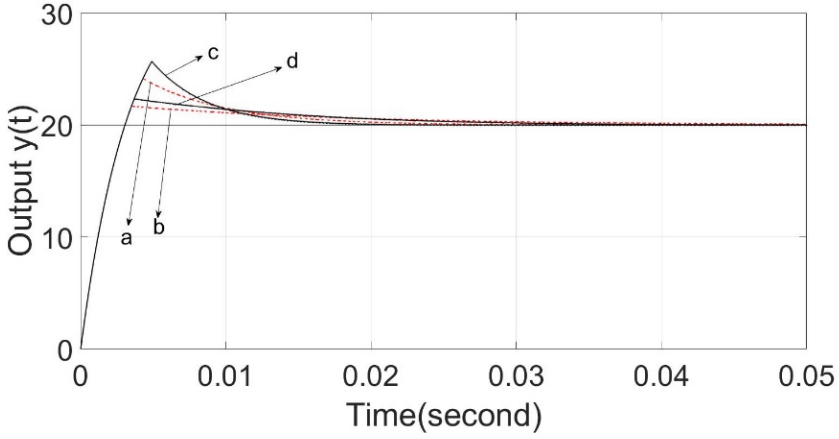

Figure. 3-5. The Responses for Conventional PID Control System with Fixed K_p, K_d and Different K_i. (a) $\xi = 0.6, K_i = 173$, (b) $\xi = 0.707, K_i = 125$, (c) $\xi = 1, K_i = 62.6$, (d) $\xi = 1.2, K_i = 43.5$.

3.2.3 New Digital PID Controller Design of DC-DC Buck Converter

Based on the parameters $L = 2mH, C = 20\mu F, R = 0.5\Omega, v_{in} = 40V, D = 0.5$, the transfer function of converter is:

$$G_{buck}(s) = \frac{K_2 K_3 v_{in}}{s^2 + sK_4 + K_2 K_3} = \frac{1\times10^9}{s^2 + 1\times10^5 s + 2.5\times10^7} \tag{3.24}$$

The transfer function of DC-DC Buck converter can be transferred form continues time domain to discrete time domain by using zero order hold method and the sampling time is 0.00001s. The Laplace transform transfer function of the Zero Order Hold is:

$$G_h(s) = \frac{1 - e^{-sT_s}}{s} \tag{3.25}$$

$H(s)$ is:

$$H(z) = \frac{G_p(s)}{1 + K_p G_p(s)} = \frac{1\times10^9}{s^2 + 1\times10^5 s + 2.5\times10^7 + 1\times10^9 K_p} \tag{3.26}$$

The discrete $H(z)$ can be obtained by using Z-transform on the plant $G_{hp}(s)$ with sampling time $T_s = 0.00001s$:

$$H(z)=\frac{G_p(z)}{1+K_pG_p(z)}=\frac{0.03678z+0.02642}{z^2+(0.03678K_p-1.366)z+0.02642K_p+0.3679} \tag{3.27}$$

The lead-phase compensator $G_f(z)$ can be written as:

$$G_f(z)=\frac{1}{H(z)}=\frac{z^2+(0.03678K_p-1.366)z+0.02642K_p+0.3679}{0.03678z+0.02642} \tag{3.28}$$

The new integral term is composed by the combination of lead-phase compensator and discrete integrator. The new integral term is expressed as:

$$G_I(z)=K_I\frac{T_s}{z-1}G_f(z)=K_IT_s\frac{z^2+(0.03678K_p-1.366)z+0.02642K_p+0.3679}{0.03678z^2-0.01036z-0.02642} \tag{3.29}$$

3.2.4 Simulations and Results

a. Without the Lead-phase Compensator

In this case, the proportional and integral gain are selected as 0.1 and 30 respectively. The parameters are shown in Table 6.

Table 6. Parameters of New Design Method for Buck Converter with and without $G_f(z)$

	K_I	K_p	$G_I(z)$
With $G_f(z)$	173	0.5	$\frac{0.00173z^2-0.002331z+0.0006593}{0.03678z^2-0.01036z-0.02642}$
Without $G_f(z)$	173	0.5	$\frac{0.00173}{z-1}$

The responses are shown in Figure 3-6. The Y-axis Output y(t) denotes the output voltage.

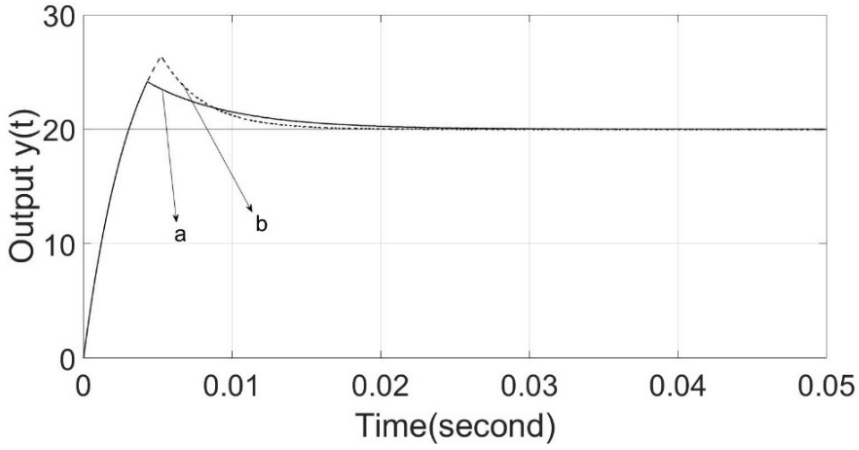

Figure. 3-6. The Responses of The System with and without Lead-phase Compensator. (a) With Lead-phase Compensator. (b) Without Lead-phase Compensator

It can be obtained that the overshoot of the closed-loop system is suppressed by the lead-phase compensator, which means the damping ratio is increased by employing lead-phase compensator. In addition, the error convergence rate becomes slowly with the lead-phase compensator.

b. Comparing Between Pole Placement PID Controller and New Digital PID Controller

In this case, the new design method is compared with pole placement method for a second order plant. The proportional gain and derivative gain are chosen as 0.5 and 0.001 respectively. The parameter ξ are selected as 0.6 and 1 The parameters for these two methods are shown in Table 7 and the responses are shown in Figure 3-7. The Y-axis Output y(t) denotes the output voltage.

Table 7. Parameters of Two Methods for Buck Converter with Fixed K_p and K_d

Design Methods	ξ	K_p	K_d	K_i
Pole Placement	0.6	0.5	0.001	173
Pole Placement	1	0.5	0.001	62.6
New Method	0.6	0.5	$G_f(z)$	173
New Method	1	0.5	$G_f(z)$	62.6

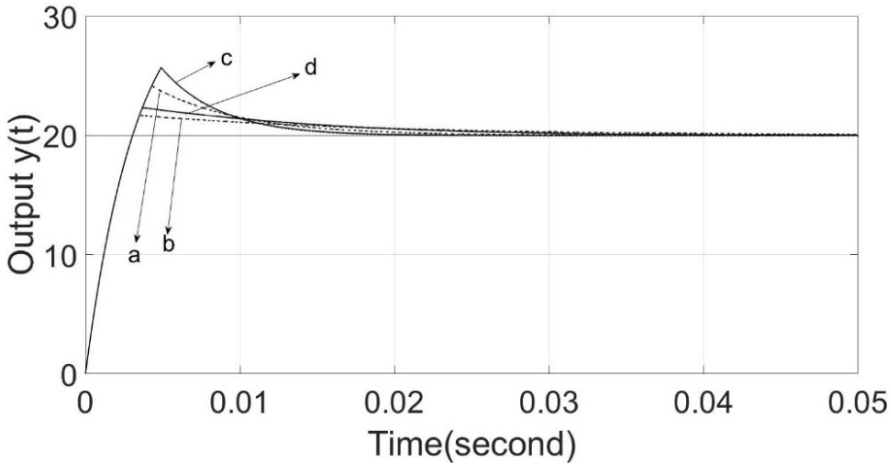

Figure. 3-7. The Comparison Between Pole Placement Method and New Design Method. (a) and (b) New Method, ξ are 0.6 and 1, K_I are 173 and 62.6 respectively. (c) and (d) Pole Placement Method, ξ are 0.6 and 1, K_I are 173 and 62.6 respectively.

Comparing a with c, b with d, it can be obtained that the overshoots for the responses are suppressed with the new digital PID controller. However, the error convergence rate of the system with new digital PID controller is degraded.

3.3 DC-DC Boost Converter

The boost converter produces higher level output voltage than dc input voltage. The mainly applications of boost converter are regulated dc power supplies and regenerative braking of dc motors. When the switch is on, the output stage is isolated, the inductor stores energy from power source in the form of magnetic field. When the switch is off, the inductor becomes a power source to maintain the current flow towards to the load, and the polarity will be reversed. So that the inductor and the dc power source can be considered as two sources which are connected in series, which leads to a higher voltage to charge the capacitor. So that the output voltage (capacitor voltage or load voltage) will be higher than input voltage.

3.3.1 Small Signal Modelling of DC-DC Boost Converter

The circuit of a DC-DC Boost converter is shown in Figure 3-8.

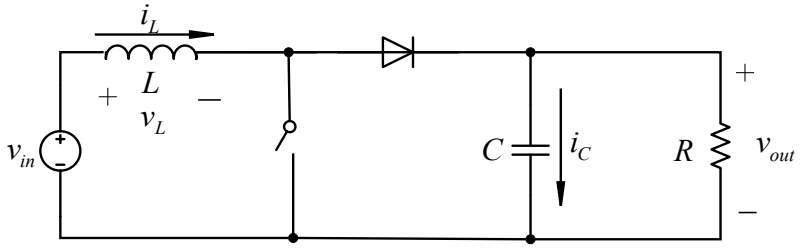

Figure.3-8. The Circuit of Boost Converter

When the switch is turned on, the circuit is shown in Figure 3-9.

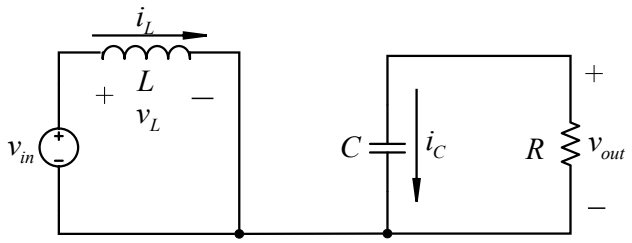

Figure. 3-9. The Circuit of Boost Converter when Switch is Turned On

the state space equation is:

$$\begin{bmatrix} \frac{di_L(t)}{dt} \\ \frac{dv_{out}(t)}{dt} \end{bmatrix} = \begin{bmatrix} 0 & 0 \\ 0 & -\frac{1}{RC} \end{bmatrix} \begin{bmatrix} i_L(t) \\ v_{out}(t) \end{bmatrix} + \begin{bmatrix} \frac{1}{L} \\ 0 \end{bmatrix} v_{in} \tag{3.30}$$

When the switch is off, the circuit is shown in Figure 3-10.

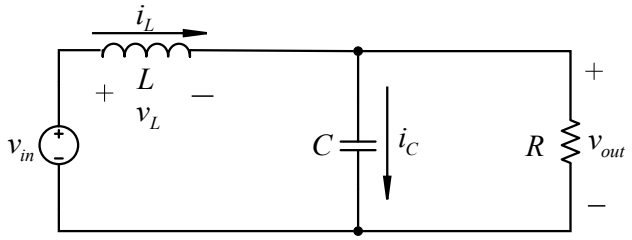

Figure. 3-10. The Circuit of Boost Converter when Switch is Turned Off

the state space equation becomes:

$$\begin{bmatrix} \frac{di_L(t)}{dt} \\ \frac{dv_{out}(t)}{dt} \end{bmatrix} = \begin{bmatrix} 0 & -\frac{1}{L} \\ \frac{1}{C} & -\frac{1}{RC} \end{bmatrix} \begin{bmatrix} i_L(t) \\ v_{out}(t) \end{bmatrix} + \begin{bmatrix} \frac{1}{L} \\ 0 \end{bmatrix} v_{in} \tag{3.31}$$

Let the duty cycle as d, the averaging state space equation of the inductor voltage and capacitor current can be expressed as:

$$\begin{bmatrix} \frac{di_L(t)}{dt} \\ \frac{dv_{out}(t)}{dt} \end{bmatrix} = \begin{bmatrix} 0 & -\frac{1-d}{L} \\ \frac{1-d}{C} & -\frac{1}{RC} \end{bmatrix} \begin{bmatrix} i_L(t) \\ v_{out}(t) \end{bmatrix} + \begin{bmatrix} \frac{1}{L} \\ 0 \end{bmatrix} v_{in} \tag{3.32}$$

Thus, we have:

$$\begin{cases} \frac{di_L(t)}{dt} = \frac{1}{L} v_{in} - \frac{1-d}{L} v_{out}(t) \\ \frac{dv_{out}(t)}{dt} = \frac{1-d}{C} i_L(t) - \frac{1}{RC} v_{out}(t) \end{cases} \tag{3.33}$$

The average state variables can be decomposed into the combination of steady-state component and AC small perturbations, which is:

$$\begin{aligned} i_L(t) &= I_L + \hat{i}_L(t) \\ v_{in} &= V_{in} + \hat{v}_{in}(t) \\ v_{out}(t) &= V_{out} + \hat{v}_{out}(t) \\ d &= D + \hat{d}(t) \end{aligned} \tag{3.34}$$

The differential equations of the small signal model are:

$$\begin{cases} \dfrac{d(\hat{i}_L(t) + I_L)}{dt} = \dfrac{1}{L}(V_{in} + \hat{v}_{in}(t)) - \dfrac{1 - D - \hat{d}(t)}{L}(V_{out} + \hat{v}_{out}(t)) \\ \dfrac{d(V_{out} + \hat{v}_{out}(t))}{dt} = \dfrac{1 - D - \hat{d}(t)}{C}(I_L + \hat{i}_L(t)) - \dfrac{1}{RC}(V_{out} + \hat{v}_{out}(t)) \end{cases} \tag{3.35}$$

Ignoring the DC component and high order items, we have:

$$\begin{cases} \dfrac{d\hat{i}_L(t)}{dt} = \dfrac{1}{L}\hat{v}_{in}(t) - \dfrac{1}{L}(1 - D)\hat{v}_{out}(t) + \dfrac{1}{L}\hat{d}(t)V_{out} \\ \dfrac{d\hat{v}_{out}(t)}{dt} = \dfrac{1}{C}(1 - D)\hat{i}_L(t) - \dfrac{1}{RC}\hat{v}_{out}(t) - \dfrac{1}{C}\hat{d}(t)I_L \end{cases} \tag{3.36}$$

The small signal equivalent circuit of DC-DC Boost Converter is:

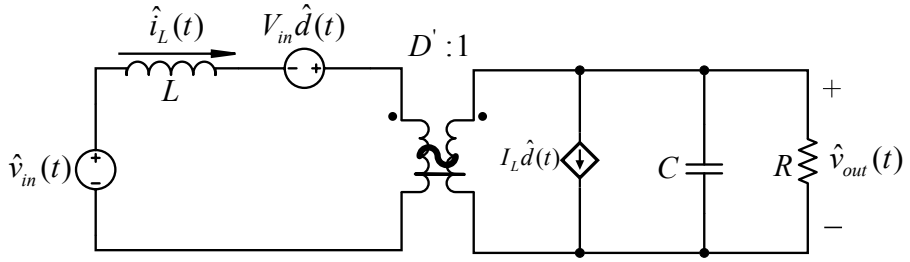

Figure. 3-11. The Small Signal Model of Boost Converter

Using Laplace transform, we have:

$$\begin{cases} s\dfrac{d\hat{i}_L(s)}{dt} = \dfrac{1}{L}\hat{v}_{in}(s) - \dfrac{1}{L}(1-D)\hat{v}_{out}(s) + \dfrac{1}{L}\hat{d}(s)V_{out} \\ s\dfrac{d\hat{v}_{out}(s)}{dt} = \dfrac{1}{C}(1-D)\hat{i}_L(s) - \dfrac{1}{RC}\hat{v}_{out}(s) - \dfrac{1}{C}\hat{d}(s)I_L \end{cases} \tag{3.37}$$

Based on the circuit diagram of Boost converter, we have:

$$\begin{cases} \dfrac{V_{out}}{V_{in}} = \dfrac{1}{D'} \\ I_L = \dfrac{V_{in}}{D'R} \end{cases} \tag{3.38}$$

According to the circuit, the transfer function between the output voltage and duty cycle is:

$$G_{vd}(s) = \left.\frac{\hat{v}_{out}(s)}{\hat{d}(s)}\right|_{v_{in}(s)=0} = \frac{V_{in}}{(1-D)^2}\frac{\dfrac{(1-D)^2}{LC} - s\dfrac{1}{RC}}{s^2 + s\dfrac{1}{RC} + \dfrac{(1-D)^2}{LC}} \tag{3.39}$$

Let:

$$D' = 1-D, F_1 = \frac{1}{R}, F_2 = \frac{1}{C}, F_3 = \frac{1}{L} \tag{3.40}$$

The transfer function becomes:

$$G_{boost}(s) = \frac{V_{in}F_2F_3 - s\dfrac{V_{in}F_1F_2}{D'^2}}{s^2 + sF_1F_2 + D'^2F_2F_3} \tag{3.41}$$

3.3.2 Conventional PID Controller Design of DC-DC Boost Converter

In this report, a conventional PID controller is designed based on the pole placement method. The transfer function of a conventional PID controller is:

$$G_L(s) = K_p + K_i \frac{1}{s} + K_d s \tag{3.42}$$

The transfer function of a conventional PID control system is:

$$G_m(s) = \frac{G_L(s)G_{vd}(s)}{1 + G_L(s)G_{vd}(s)} \tag{3.43}$$

The characteristic equation of $G_m(s)$ is:

$$s^3 + s^2\left(\frac{D'^2F_1F_2 + D'^2V_{in}F_2F_3K_d - V_{in}F_1F_2K_p}{D'^2 - V_{in}F_1F_2K_d}\right) + s\left(\frac{D'^4F_2F_3 + D'^2V_{in}F_2F_3K_p - V_{in}F_1F_2K_i}{D'^2 - V_{in}F_1F_2K_d}\right) + \frac{D'^2V_{in}F_2F_3K_i}{D'^2 - V_{in}F_1F_2K_d} \tag{3.44}$$

A suitable closed-loop characteristic equation of a third order system can be written as:

$$(s + \alpha\omega_n)(s^2 + 2\xi\omega_n s + \omega_n{}^2) = 0 \tag{3.45}$$

where ξ and ω_n denote the damping ratio and natural frequency respectively. α is a constant. We have:

$$\begin{aligned}
&\frac{D^{'2}F_1F_2 + D^{'2}V_{in}F_2F_3K_d - V_{in}F_1F_2K_p}{D^{'2} - V_{in}F_1F_2K_d} = \omega_n(\alpha + 2\xi) \\
&\frac{D^{'4}F_2F_3 + D^{'2}V_{in}F_2F_3K_p - V_{in}F_1F_2K_i}{D^{'2} - V_{in}F_1F_2K_d} = \omega_n{}^2(1 + 2\xi\alpha) \\
&\frac{D^{'2}V_{in}F_2F_3K_i}{D^{'2} - V_{in}F_1F_2K_d} = \alpha\omega_n{}^3
\end{aligned} \tag{3.46}$$

In this case, $L = 100\mu H, C = 1mF, R = 300\Omega, v_{in} = 80, D^{'} = 0.8$. The proportional gain and derivative gain are fixed as 0.03 and 0.0001 respectively. We have:

$$F_1 = 0.00333, F_2 = 1000, F_3 = 10000$$

The values of ξ are 0.6, 0.707, 1 and 1.2 respectively, and the reference output voltage is set as 100v. The parameters for Boost Converter and PID controller are shown in Table 8 and Table 9.

Table 8. The Parameters for Boost Converter

$L(H)$	1×10^{-4}
$C(F)$	1×10^{-3}
$R(\Omega)$	300
$V_{in}(V)$	80
$V_{out}(V)$	100
D	0.2

Table 9. Parameters of Conventional PID Controller for Boost Converter with Fixed K_p, K_d

K_p	K_d	K_i	ξ	$\omega_n(rad/s)$	α
0.03	0.0001	10	0.6	317.117	262.01173

0.03	0.0001	7.2223	0.707	269.3734	308.45
0.03	0.0001	3.6187	1	190.6753	435.754
0.03	0.0001	2.5148	1.2	158.9544	522.7128

The responses are shown in Figure. 3-12. The Y-axis Output y(t) denotes the output voltage.

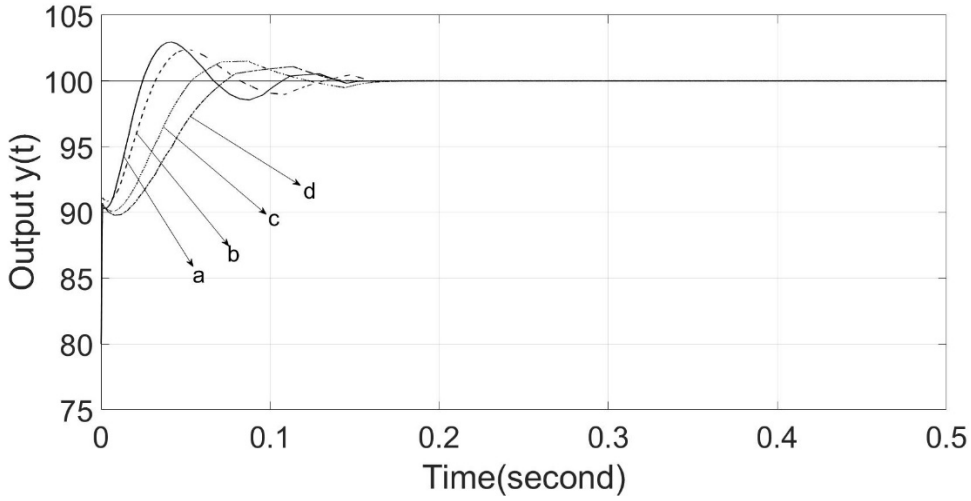

Figure. 3-12. The Responses for Conventional PID Control System with Fixed K_p, K_d and Different K_i. (a) $\xi = 0.6, K_i = 10$, (b) $\xi = 0.707, K_i = 7.2223$, (c) $\xi = 1, K_i = 3.6187$, (d) $\xi = 1.2, K_i = 2.5148$.

3.3.3 New Digital PID Controller Design of DC-DC Boost Converter (Non-minimum-Phase System)

The Laplace transform of the Boost converter is:

$$G_{boost}(s) = \frac{-416.7s + 8\times10^8}{s^2 + 3.333s + 6.4\times10^6} \tag{3.47}$$

According to the transfer function of boost converter, the zero is located at the right half plane, which means the boost converter is a non-minimum-phase system (NMP). The lead-

phase compensator $G_f(z)$ which is based on the model inverse technique will be unstable because the pole is outside the unit circle. Such problem can be solved by designing the approximate inverse model. There are three stable approximate model-inverse control techniques to approximate the inverse. The non-minimum-phase zeros ignore (NPZ-ignore), the zero-phase-error tracking controller (ZPETC) and zero-magnitude-error tracking controller (ZMETC). Such three methods are analysed and compared by J.A. Butterworth [26]. When using NPZ-ignore method, the designers ignore all non-minimum phase zeros. Such method is simplest, however, the precise is the worst. ZPETC and ZMETC retain the dynamics of NMP zeros. The difference between these two methods is, the ZPETC converts the NMP zeros into stable zeros of the approximate inverse, the ZMETC transforms the NMP zeros into stable poles of the inverse model. The NMP-ignore method is not considered in this report due to the unsatisfactory precise. The redesigned integrator $G_I(z)$ non-causal by using ZPETC. In this report, the ZMETC technique is selected to approximate the inverse model. As mentioned before, the transfer function $H(z)$ can be described as:

$$H(z) = \frac{G_p(z)}{1 + K_p G_p(z)} = \frac{B(z)}{A(z)} = \frac{z^{-d} B^+(z) B^-(z)}{A(z)} \tag{3.48}$$

$B^-(z)$ contains the roots on or outside the unit circle and undesired roots, and it can be described in the form of the n^{th} order polynomial as:

$$B^-(z) = B_n^- z^n + B_{n-1}^- z^{n-1} + \ldots + B_0^- \tag{3.49}$$

where n denotes the number of the NMP zeros. The approximate inverse model of $H(z)$ can be written as:

$$\tilde{H(z)}^{-1} = \frac{z^d A(z)}{B^+(z) B^{-*}(z)} \tag{3.50}$$

$\tilde{H(z)}^{-1}$ represents the approximate inverse model, $B^{-*}(z)$ is designed as below by using ZMETC method:

$$B^{-*}(z) = B_0^- z^n + B_1^- z^{n-1} + ... + B_n^- \tag{3.51}$$

In this case, the sampling time is 0.00001s and the transfer function of $H(z)$ is:

$$H(z) = \frac{G_p(z)}{1 + K_p G_p(z)} = \frac{-1.667 \times 10^{-5} z + 0.0008167}{z^2 - (1.667 \times 10^{-5} K_p + 1.991)z + 0.0008167 K_p + 0.991} \tag{3.52}$$

where $B^-(z)$ is:

$$B^-(z) = -1.667 \times 10^{-5} z + 0.0008167 \tag{3.53}$$

So that $B^{-*}(z)$ can be written as:

$$B^{-*}(z) = 0.0008167z - 1.667 \times 10^{-5} \tag{3.54}$$

The lead-phase compensator $G_f(z)$ which is the approximate inverse of $H(z)$ can be designed by using ZMETC as:

$$G_f(z) = \frac{z^2 - (1.667 \times 10^{-5} K_p + 1.991)z + 0.0008167 K_p + 0.991}{0.0008167z - 1.667 \times 10^{-5}} \tag{3.55}$$

The new integral term is composed by the combination of lead-phase compensator and discrete integrator. The new integral term is expressed as:

$$G_I(z) = K_I \frac{T_s}{z-1} G_f(z) = K_I T_s \frac{z^2 - (1.667\times10^{-5}K_p + 1.991)z + 0.0008167K_p + 0.991}{0.0008167z^2 - 0.00083337z + 1.667\times10^{-5}} \quad (3.56)$$

3.3.4 Simulations and Results

a. Without the Lead-phase Compensator

In this case, the proportional and integral gain are selected as 0.002 and 10 respectively. The parameters are shown in Table 10.

Table 10. Parameters of New Design Method for Boost Converter with and without $G_f(z)$

	K_I	K_p	$G_I(z)$
With $G_f(z)$	20	0.03	$\frac{2\times10^{-5}z^2 - 3.982\times10^{-5}z + 1.982\times10^{-5}}{0.0008165z^2 - 0.0008332z - 1.667\times10^{-5}}$
Without $G_f(z)$	20	0.03	$\frac{0.00002}{z-1}$

The responses are shown in Figure. 3-13. The Y-axis Output y(t) denotes the output voltage.

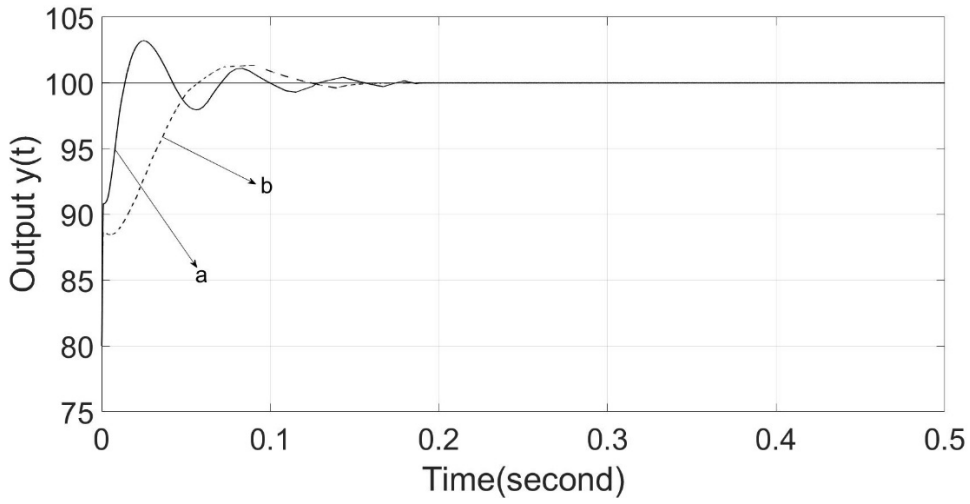

Figure. 3-13. The Responses of The System with and without Lead-phase Compensator. (a) Without Lead-phase Compensator. (b) With Lead-phase Compensator

It can be obtained that the overshoot of the closed-loop system is suppressed by the lead-phase compensator, which means the damping ratio is increased by employing lead-phase compensator. However, the error convergence rate is slow with the lead-phase compensator.

b. Comparing Between Pole Placement PID Controller and New Digital PID Controller

In this case, the proportional gain and derivative gain are chosen as 0.002 and 0.00001 respectively. The parameter ξ are selected as 0.6 and 0.707. The parameters for these two methods are shown in Table 11 and the responses are shown in Figure. 3-14. The Y-axis Output y(t) denotes the output voltage.

Table 11. Parameters of Two Methods for Boost Converter with Fixed K_p and K_d

Design Methods	K_p	K_d	K_i
Pole Placement	0.002	0.00001	0.675
Pole Placement	0.002	0.00001	0.4937
New Method	0.002	$G_f(z)$	0.675
New Method	0.002	$G_f(z)$	0.4937

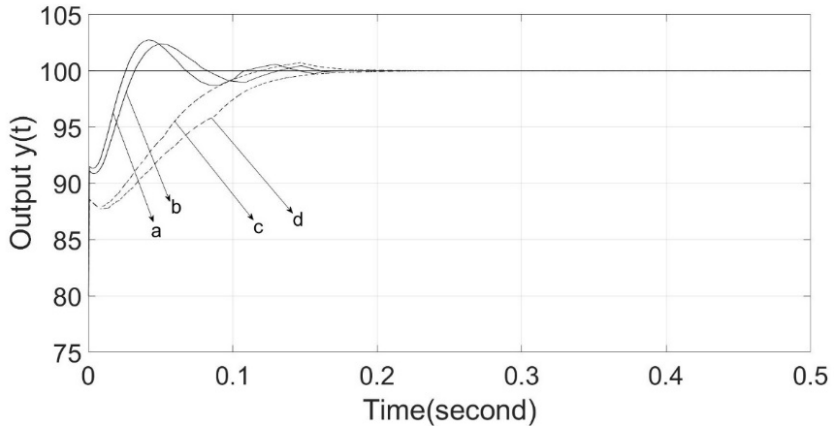

Figure. 3-14. The Comparison Between Pole Placement Method and New Design Method. (a) and (b) are Pole Placement method K_I are 10 and 7.2223. (c) and (d) are New Method, K_I are 10 and 7.2223.

Comparing a with c, b with d, it can be obtained that the overshoot is suppressed significantly with the help of new digital PID controller. However, the rise time is larger, and the error convergence rate is slower.

3.4 DC-DC Buck-Boost Converter

The Buck-Boost converter can produce either higher or lower output voltage. It is mainly employed in regulated dc power supplies. The output voltage is desired as negative polarity with respect to the common terminal of the input voltage. The buck-boost converter can be considered as the cascade combination of two basic converters (buck, boost converter). When the switch is on, the diode is reverse biased, and the inductor stores the energy from the input power source. In addition, the capacitor provides energy to load. When the switch is opened, the input power source is removed from the circuit, the inductor provides energy to the load.

3.4.1 Small Signal Modelling of DC-DC Buck-Boost Converter

The diagram of the Buck-Boost Converter is shown in Figure 3-15.

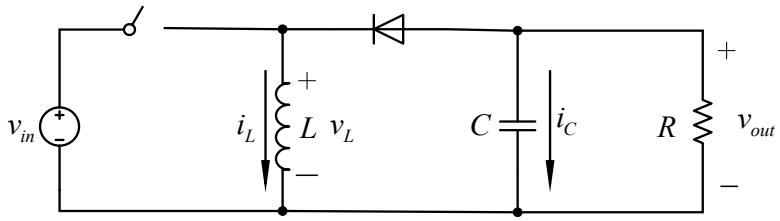

Figure. 3-15. The Circuit of Buck-Boost Converter

When the switch is turned on, the circuit is shown in Figure 3-16.

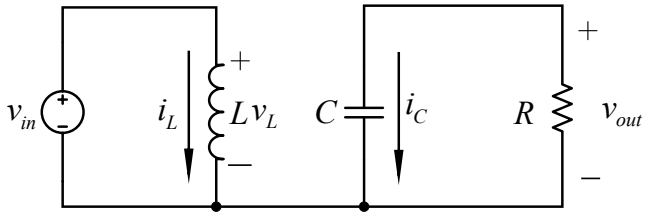

Figure. 3-16. The Circuit of Buck-Boost Converter when the Switch is Turned On

The inductor voltage and capacitor current are:

$$\begin{bmatrix} \frac{di_L(t)}{dt} \\ \frac{dv_{out}(t)}{dt} \end{bmatrix} = \begin{bmatrix} 0 & 0 \\ 0 & -\frac{1}{RC} \end{bmatrix} \begin{bmatrix} i_L(t) \\ v_{out}(t) \end{bmatrix} + \begin{bmatrix} \frac{1}{L} \\ 0 \end{bmatrix} v_{in} \tag{3.57}$$

When the switch is turned off, the circuit is shown in Figure 3-17.

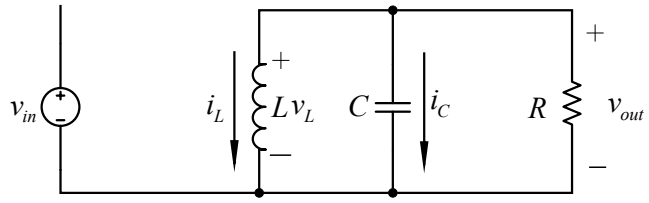

Figure. 3-17. The Circuit of Buck-Boost Converter when the Switch is Turned Off

The inductor voltage and capacitor current are:

$$\begin{bmatrix} \frac{di_L(t)}{dt} \\ \frac{dv_{out}(t)}{dt} \end{bmatrix} = \begin{bmatrix} 0 & \frac{1}{L} \\ -\frac{1}{C} & -\frac{1}{RC} \end{bmatrix} \begin{bmatrix} i_L(t) \\ v_{out}(t) \end{bmatrix} + \begin{bmatrix} 0 \\ 0 \end{bmatrix} v_{in} \tag{3.58}$$

Based on above, the state-space averaging model of Buck-Boost Converter is:

$$\begin{bmatrix} \frac{di_L(t)}{dt} \\ \frac{dv_{out}(t)}{dt} \end{bmatrix} = \begin{bmatrix} 0 & \frac{1-d}{L} \\ -\frac{1-d}{C} & -\frac{1}{RC} \end{bmatrix} \begin{bmatrix} i_L(t) \\ v_{out}(t) \end{bmatrix} + \begin{bmatrix} \frac{d}{L} \\ 0 \end{bmatrix} v_{in} \tag{3.59}$$

The differential equations of inductor voltage and capacitor current are:

$$\begin{cases} \frac{di_L(t)}{dt} = \frac{d}{L} v_{in} + \frac{1-d}{L} v_{out}(t) \\ \frac{dv_{out}(t)}{dt} = -\frac{1-d}{C} i_L(t) - \frac{1}{RC} v_{out}(t) \end{cases} \tag{3.60}$$

Similar as before, constructing the small signal model, the inductor voltage, capacitor current and duty cycle can be decomposed into the steady-state components and AC perturbations as below:

$$\begin{aligned} i_L(t) &= I_L + \hat{i}_L(t) \\ v_{in} &= V_{in} + \hat{v}_{in}(t) \\ v_{out}(t) &= V_{out} + \hat{v}_{out}(t) \\ d &= D + \hat{d}(t) \end{aligned} \tag{3.61}$$

The differential equations of the small signal model are:

$$\begin{cases} \frac{d(\hat{i}_L(t) + I_L)}{dt} = \frac{D + \hat{d}(t)}{L} (V_{in} + \hat{v}_{in}(t)) + \frac{1 - D - \hat{d}(t)}{L} (V_{out} + \hat{v}_{out}(t)) \\ \frac{d(V_{out} + \hat{v}_{out}(t))}{dt} = -\frac{1 - D - \hat{d}(t)}{C} (I_L + \hat{i}_L(t)) - \frac{1}{RC} (V_{out} + \hat{v}_{out}(t)) \end{cases} \tag{3.62}$$

Ignoring the DC component and high order items, we have:

$$\begin{cases} \dfrac{d\hat{i}_L(t)}{dt} = \dfrac{D}{L}\hat{v}_{in}(t) + \dfrac{1}{L}(1-D)\hat{v}_{out}(t) + \dfrac{1}{L}\hat{d}(t)(V_{in} - V_{out}) \\ \dfrac{d\hat{v}_{out}(t)}{dt} = -\dfrac{1}{C}(1-D)\hat{i}_L(t) - \dfrac{1}{RC}\hat{v}_{out}(t) - \dfrac{1}{C}\hat{d}(t)I_L \end{cases} \tag{3.63}$$

The small signal equivalent circuit of DC-DC Boost Converter is shown in Figure 3-18.

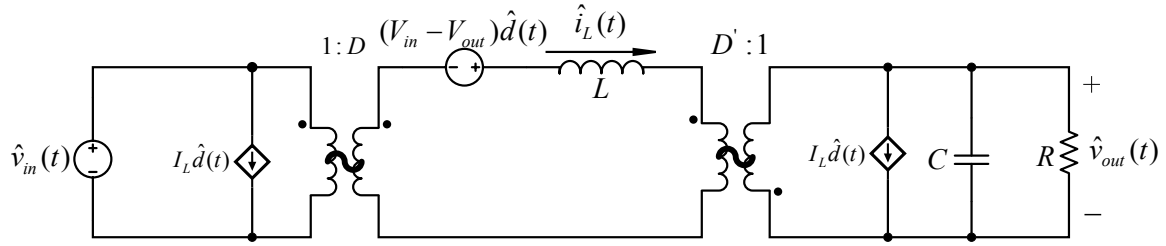

Figure. 3-18. The Small Signal Model of Buck-Boost Converter

Using Laplace transform, we have:

$$\begin{cases} s\hat{i}_L(s) = \dfrac{D}{L}\hat{v}_{in}(s) + \dfrac{1}{L}(1-D)\hat{v}_{out}(s) + \dfrac{1}{L}\hat{d}(s)(V_{in} - V_{out}) \\ s\hat{v}_{out}(s) = -\dfrac{1}{C}(1-D)\hat{i}_L(s) - \dfrac{1}{RC}\hat{v}_{out}(s) - \dfrac{1}{C}\hat{d}(s)I_L \end{cases} \tag{3.64}$$

According to the circuit, we have:

$$\begin{cases} \dfrac{V_{out}}{R} = -I_L(1-D) \\ V_{out} = -\dfrac{D}{D'}V_{in} \end{cases} \tag{3.65}$$

where $D' = 1 - D$. The transfer function between output voltage and duty cycle is:

$$G_{vd}(s)=\left.\frac{\hat{v}_{out}(s)}{\hat{d}(s)}\right|_{v_{in}(s)=0}=\frac{\frac{V_{in}D^{'}}{LCD}-\frac{sV_{in}}{D^{'}RC}}{s^2+s\frac{1}{RC}+\frac{D^{'2}}{LC}} \tag{3.66}$$

Let

$$F_1=\frac{1}{R},F_2=\frac{1}{C},F_3=\frac{1}{L} \tag{3.67}$$

We have the transfer function as:

$$G_{vd}(s)=\left.\frac{\hat{v}_{out}(s)}{\hat{d}(s)}\right|_{v_{in}(s)=0}=\frac{F_2F_3\frac{V_{in}D^{'}}{D}-F_1F_2\frac{sV_{in}}{D^{'}}}{s^2+sF_1F_2+F_2F_3D^{'2}} \tag{3.68}$$

3.4.2 The Conventional PID Controller Design of Buck-Boost Converter

In this report, a conventional PID controller is designed based on the pole placement method. The transfer function of a conventional PID controller is:

$$G_L(s)=K_p+K_i\frac{1}{s}+K_ds \tag{3.69}$$

The transfer function of a conventional PID control system is:

$$G_m(s) = \frac{G_L(s)G_{vd}(s)}{1 + G_L(s)G_{vd}(s)} \tag{3.70}$$

The characteristic equation of $G_m(s)$ is:

$$s^3 + s^2\left(\frac{D^{'}F_1F_2 + \frac{V_{in}D^{'2}}{D}F_2F_3K_d - V_{in}F_1F_2K_p}{D^{'} - V_{in}F_1F_2K_d}\right) + s\left(\frac{D^{'3}F_2F_3 + \frac{V_{in}D^{'2}}{D}F_2F_3K_p - V_{in}F_1F_2K_i}{D^{'} - V_{in}F_1F_2K_d}\right) + \frac{\frac{V_{in}D^{'2}}{D}F_2F_3K_i}{D^{'} - V_{in}F_1F_2K_d} \tag{3.71}$$

A suitable closed-loop characteristic equation of a third order system can be written as:

$$(s + \alpha\omega_n)(s^2 + 2\xi\omega_n s + \omega_n{}^2) = 0 \tag{3.72}$$

where ξ and ω_n denote the damping ratio and natural frequency respectively. α is a constant. We have:

$$\begin{aligned}
&\frac{D^{'}F_1F_2 + \frac{V_{in}D^{'2}}{D}F_2F_3K_d - V_{in}F_1F_2K_p}{D^{'} - V_{in}F_1F_2K_d} = \omega_n(\alpha + 2\xi) \\
&\frac{D^{'3}F_2F_3 + \frac{V_{in}D^{'2}}{D}F_2F_3K_p - V_{in}F_1F_2K_i}{D^{'} - V_{in}F_1F_2K_d} = \omega_n{}^2(1 + 2\xi\alpha) \\
&\frac{\frac{V_{in}D^{'2}}{D}F_2F_3K_i}{D^{'} - V_{in}F_1F_2K_d} = \alpha\omega_n{}^3
\end{aligned} \tag{3.73}$$

In this case, $L = 100\mu H, C = 500\mu F, R = 50\Omega, v_{in} = 40, D^{'} = 0.9$. The proportional gain and derivative gain are fixed as 0.002 and 0.00001 respectively, the sampling time is set as 0.00001s. We have:

$$F_1 = 0.02, F_2 = 10000, F_3 = 2000$$

The values of ξ are 0.6, 0.707, 1 and 1.2 respectively, and the reference output voltage is set as 5v. The parameters for Buck-Boost converter and PID controller are shown in Table 12 and 13 respectively.

Table 12. The Parameters for Buck-Boost Converter

$L(H)$	1×10^{-4}
$C(F)$	5×10^{-4}
$R(\Omega)$	50
$V_{in}(V)$	40
$V_{out}(V)$	5
D	0.1

Table 13. Parameters of Conventional PID Controller for Buck-Boost Converter with Fixed K_p, K_d

K_p	K_d	K_i	ξ	$\omega_n(rad/s)$	α
0.002	0.00001	1.251	0.6	354.6	205.63
0.002	0.00001	0.9028	0.707	301.3	242.02
0.002	0.00001	0.4526	1	213.32	341.8
0.002	0.00001	0.3146	1.2	177.8465	410

The responses are shown in Figure 3-19. The Y-axis Output y(t) denotes the output voltage.

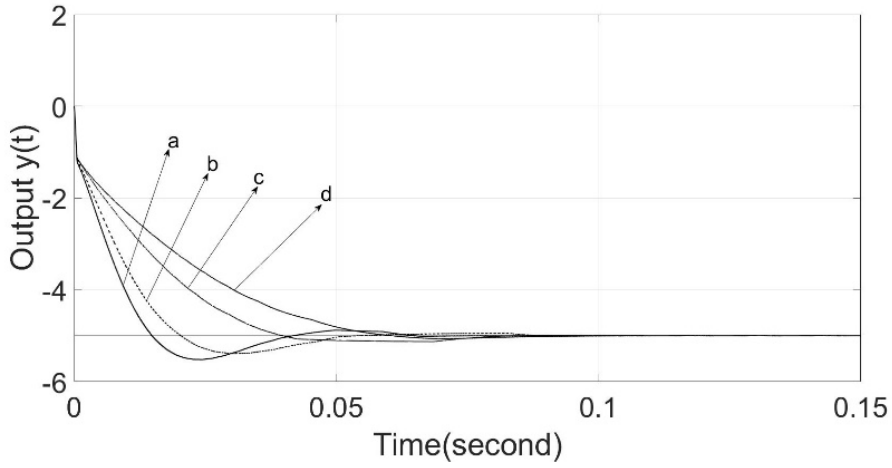

Figure. 3-19. The Responses of Conventional PID Control System for Buck-Boost Converter with Fixed K_p, K_d and Different K_i. (a) $\xi = 0.6, K_i = 1.251$, (b) $\xi = 0.707, K_i = 0.9028$, (c) $\xi = 1, K_i = 0.4526$, (d) $\xi = 1.2, K_i = 0.3146$

3.4.3 New Digital PID Controller Design of DC-DC Buck-Boost Converter (Non-minimum-Phase System)

The Laplace transform of the Boost converter is:

$$G_{buck-boost}(s) = \frac{-1778s + 7.2\times10^9}{s^2 + 40s + 1.62\times10^7} \tag{3.74}$$

Similar as Boost converter, the NMP system can be approximated by using ZMETC with sampling time as 0.00001s. In this case, the transfer function of $H(z)$ is:

$$H(z) = \frac{G_{buck-boost}(z)}{1 + K_p G_{buck-boost}(z)} = \frac{-0.0001418z + 0.0002138}{z^2 - (0.0001418K_p + 2)z + 0.0002138K_p + 1} \tag{3.75}$$

The lead-phase compensator $G_f(z)$ which is the approximate inverse of $H(z)$ can be designed by using ZMETC

$$G_f(z) = \frac{z^2 - (0.0001418K_p + 2)z + 0.0002138K_p + 1}{0.0002138z - 0.0001418} \tag{3.76}$$

The new integral term is composed by the combination of lead-phase compensator and discrete integrator. The new integral term is expressed as:

$$G_I(z) = K_I \frac{T_s}{z-1} G_f(z) = K_I T_s \frac{z^2 - (0.0001418K_p + 2)z + 0.0002138K_p + 1}{0.0002138z^2 - 0.0003556z + 0.0001418} \tag{3.77}$$

a. Without the Lead-phase Compensator

In this case, the proportional and integral gain are selected as 0.002 and 1.251 respectively. The parameters are shown in Table 14.

Table 14. Parameters of New Design Method for Buck-Boost Converter with and without $G_f(z)$

	K_I	K_p	$G_I(z)$
With $G_f(z)$	1.251	0.002	$\frac{1.251\times10^{-7}z^2 - 2.5\times10^{-7}z + 1.249\times10^{-7}}{0.0002138z^2 - 0.0003556z - 0.0001418}$
Without $G_f(z)$	1.251	0.002	$\frac{1.251\times10^{-7}}{z-1}$

The responses are shown in Figure 3-20. The Y-axis Output y(t) denotes the output voltage.

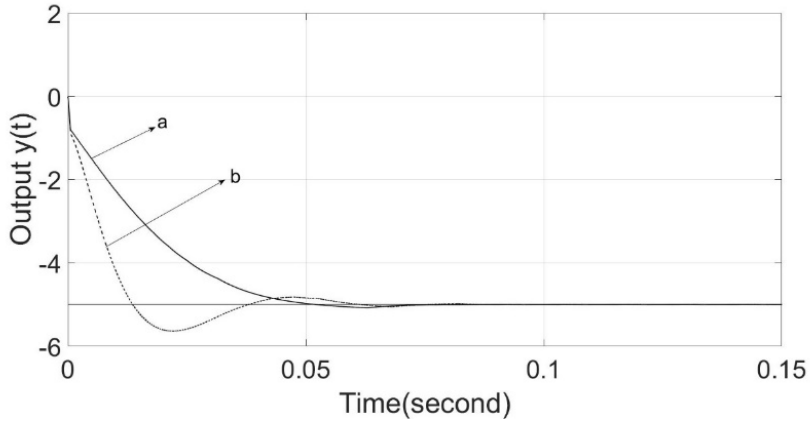

Fig. 3-20. The Responses of The System with and without Lead-phase Compensator. (a) With Lead-phase Compensator. (b) Without Lead-phase Compensator

It can be obtained that the overshoot of the closed-loop system is suppressed by the lead-phase compensator, which means the damping ratio is increased by employing lead-phase compensator. However, the rise time is larger with lead-phase compensator.

b. Comparing Between Pole Placement PID Controller and New Digital PID Controller

In this case, the proportional gain and derivative gain are chosen as 0.002 and 0.00001 respectively. The parameter ξ are selected as 0.6 and 0.707. The parameters for these two methods are shown in Table 15 and the responses are shown in Figure 3-21. The Y-axis Output y(t) denotes the output voltage.

Design Methods	K_p	K_d	K_i
Pole Placement	0.002	0.00001	0.675
Pole Placement	0.002	0.00001	0.4937
New Method	0.002	$G_f(z)$	0.675
New Method	0.002	$G_f(z)$	0.4937

Table 15. Parameters of Two Methods for Buck-Boost Converter with Fixed K_p and K_d

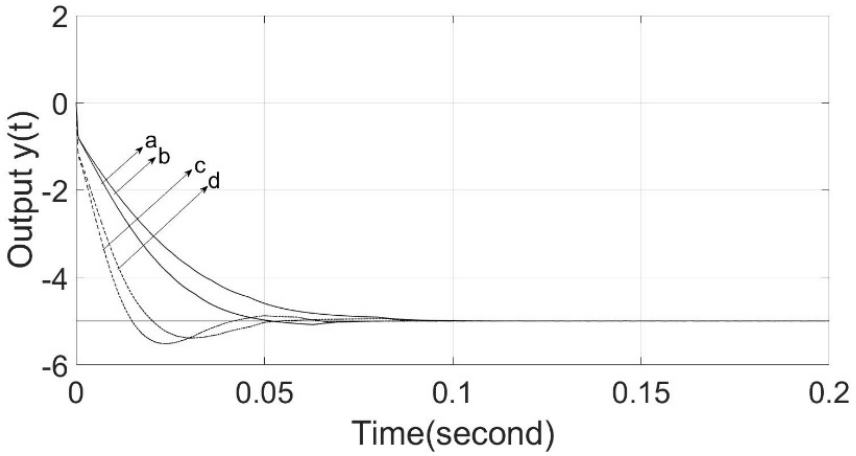

Fig. 3-21. The Comparison Between Pole Placement Method and New Design Method. (a) and (b) are New Design Method K_I are 1.251 and 0.9028. (c) and (d) are Pole Placement Method, K_I are 1.251 and 0.9028.

Comparing a with c, b with d, it can be obtained that the overshoot is suppressed significantly with new digital PID controller. However, the rise time is larger.

3.5. Summary

In this chapter, the new digital PID controller is used on DC-DC converters to demonstrate the performance. Firstly, the three kinds of DC-DC converters (buck, boost and buck-boost) are introduced and modelled. After that the conventional pole placement PID controller is designed and demonstrated with four different damping ratios. Then the new digital PID controller is designed and demonstrated with the same parameters as the pole placement method based digital PID controller. According to the simulation results, the new digital PID controller can suppress the overshoot significantly due to the lead-phase compensator. The leading phase provided by lead-phase compensator increases the damping of the system. However, the new digital PID controller makes the system “slower”, which means the rise time and the error convergence rate may become larger and slower.

4. Conclusion

4.1 General Conclusion

In this report, a new digital PID controller is proposed. The complexity of designing such new digital PID controller is less than conventional PID controller. The conventional derivative term is replaced by a lead-phase compensator and connected to the integrator in series. The stability criterion of the control system with new digital PID controller is related to the integral gain and proportional gain, which is one dimension less than conventional PID control system. In addition, the integral gain has a certain range, which means the integral gain from the range guarantees the stability of the system. Moreover, a tuning method which is related to the error convergence rate is proposed as well. Finally, some simulations are implemented to show the performance of the new digital PID controller.

According to the simulation results, the overshoot of the output signal is suppressed significantly by using new digital PID controller. However, the new digital PID controller may make the system “slower”, which means the rise time and error convergence rate may larger and slower than conventional PID control system. So that it is a trade-off between fast and small overshoot for the designers.

4.3 Future Work

Due to the time limitation, the demonstrations of the new digital PID controller on hardware experiments are arranged in the future. The new digital PID controller is still compared with conventional PID controllers to test the performance practically.

5. Reference

[1] L. Hongmei and Y. Xiao, "Sliding-mode PID control of DC-DC converter," in *2010 5th IEEE Conference on Industrial Electronics and Applications*, 2010, pp. 730-734.

[2] V. Arikatla and J. A. A. Qahouq, "DC-DC Power Converter with digital PID controller," in *2011 Twenty-Sixth Annual IEEE Applied Power Electronics Conference and Exposition (APEC)*, 2011, pp. 327-330.

[3] R. W. Erickson and D. Maksimovic, *Fundamentals of power electronics*. Springer Science & Business Media, 2007.

[4] S. Verma, S. Singh, and A. Rao, "Overview of control Techniques for DC-DC converters," *Research Journal of Engineering Sciences ISSN,* vol. 2278, p. 9472, 2013.

[5] K. J. Åström and T. Hägglund, "The future of PID control," *Control Engineering Practice,* vol. 9, no. 11, pp. 1163-1175, 2001/11/01/ 2001.

[6] A. Kiam Heong, G. Chong, and L. Yun, "PID control system analysis, design, and technology," *IEEE Transactions on Control Systems Technology,* vol. 13, no. 4, pp. 559-576, 2005.

[7] C.-C. Y. PhD, *Autotuning of PID Controllers* (A Relay Feedback Approach). London: Springer, 2006.

[8] J. G. Ziegler and N. B. Nichols, "Optimum Settings for Automatic Controllers," *Journal of Dynamic Systems, Measurement, and Control,* vol. 115, no. 2B, pp. 220-222, 1993.

[9] G. H. Cohen and G. A. Coon, "Theoretical Consideration of Retarded Control," *Transactions of the ASME,* vol. 75, pp. 827-834, 1953.

[10] K. J. Åström and T. Hägglund, "Revisiting the Ziegler–Nichols step response method for PID control," *Journal of Process Control,* vol. 14, no. 6, pp. 635-650, 2004/09/01/ 2004.

[11] K. J. Åström and T. Hägglund, *PID Controllers: Theory, Design and Tuning*, 2nd ed. International Society of Automation, 1995.

[12] P. Persson and K. J. Åström, "Dominant Pole Design - A Unified View of PID Controller Tuning," *IFAC Proceedings Volumes,* vol. 25, no. 14, pp. 377-382, 1992/07/01/ 1992.

[13] Q.-G. Wang, Z. Zhang, K. J. Astrom, and L. S. Chek, "Guaranteed dominant pole placement with PID controllers," *Journal of Process Control,* vol. 19, no. 2, pp. 349-352, 2009/02/01/ 2009.

[14] P. Cominos and N. Munro, "PID controllers: recent tuning methods and design to specification," (in English), *Iee Proceedings-Control Theory and Applications,* vol. 149, no. 1, pp. 46-53, Jan 2002.

[15] K. J. Åström and T. Hägglund, "Automatic tuning of simple regulators with specifications on phase and amplitude margins," *Automatica,* vol. 20, no. 5, pp. 645-651, 1984/09/01/ 1984.

[16] K. J. Åström, T. Hägglund, C. C. Hang, and W. K. Ho, "Automatic tuning and adaptation for PID controllers - a survey," *Control Engineering Practice,* vol. 1, no. 4, pp. 699-714, 1993/08/01/ 1993.

[17] W. K. Ho, C. C. Hang, and L. S. Cao, "Tuning of PID controllers based on gain and phase margin specifications," *Automatica,* vol. 31, no. 3, pp. 497-502, 1995/03/01/ 1995.

[18] P. D. Mandić, T. B. Šekara, M. P. Lazarević, and M. Bošković, "Dominant pole placement with fractional order PID controllers: D-decomposition approach," *ISA Transactions,* vol. 67, pp. 76-86, 2017/03/01/ 2017.

[19] Q.-G. Wang, Z. Zhang, K. J. Astrom, Y. Zhang, and Y. Zhang, "Guaranteed Dominant Pole Placement with PID Controllers," *IFAC Proceedings Volumes,* vol. 41, no. 2, pp. 5842-5845, 2008/01/01/ 2008.

[20] K. Zhou, D. Wang, Y. Yang, and F. Blaabjerg, *Periodic control of power electronic converters*. Institution of Engineering and Technology, 2017.

[21] S. Hara, Y. Yamamoto, T. Omata, and M. Nakano, "Repetitive control system: A new type servo system for periodic exogenous signals," *IEEE Transactions on automatic control,* vol. 33, no. 7, pp. 659-668, 1988.

[22] G. Hillerström and K. Walgama, "Repetitive Control Theory and Applications - A Survey," *IFAC Proceedings Volumes,* vol. 29, no. 1, pp. 1446-1451, 1996/06/01/ 1996.

[23] Z. Keliang, L. Kay-Soon, D. Wang, L. Fang-Lin, Z. Bin, and W. Yigang, "Zero-phase odd-harmonic repetitive controller for a single-phase PWM inverter," *IEEE Transactions on Power Electronics,* vol. 21, no. 1, pp. 193-201, 2006.

[24] Z. Keliang and D. Wang, "Digital repetitive controlled three-phase PWM rectifier," *IEEE Transactions on Power Electronics,* vol. 18, no. 1, pp. 309-316, 2003.

[25] B. Zhang, D. Wang, K. Zhou, and Y. Wang, "Linear phase lead compensation repetitive control of a CVCF PWM inverter," *IEEE Transactions on Industrial Electronics,* vol. 55, no. 4, pp. 1595-1602, 2008.

[26] J. Butterworth, L. Pao, and D. Abramovitch, "Analysis and comparison of three discrete-time feedforward model-inverse control techniques for nonminimum-phase systems," *Mechatronics,* vol. 22, no. 5, pp. 577-587, 2012.

6. Appendix

Some pictures of the simulation are provided in this section.

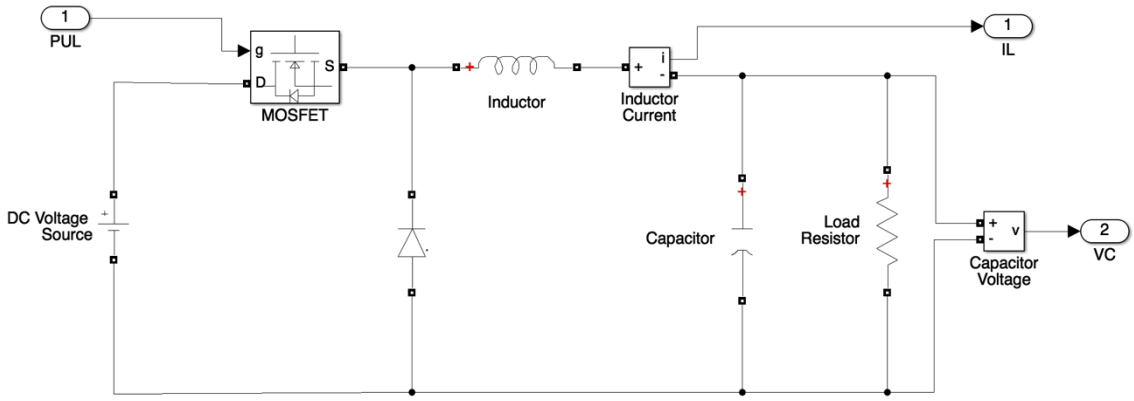

Figure 6-1. Buck converter circuit.

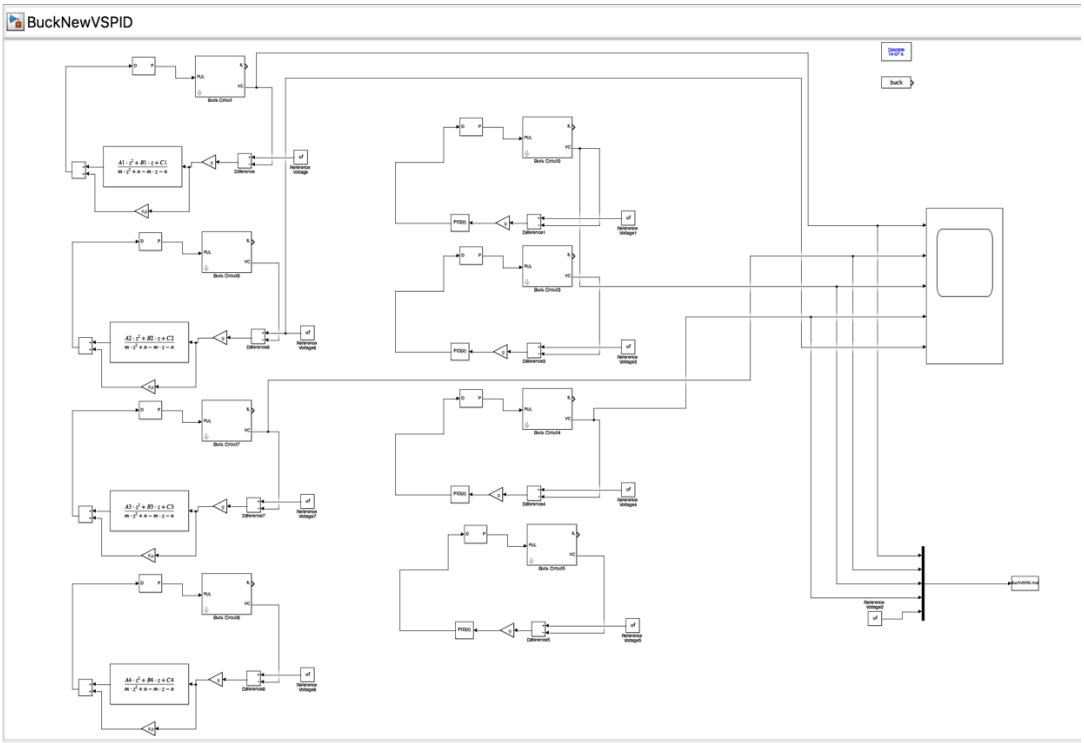

Figure 6-2. New PID VS conventional PID on Buck converter.

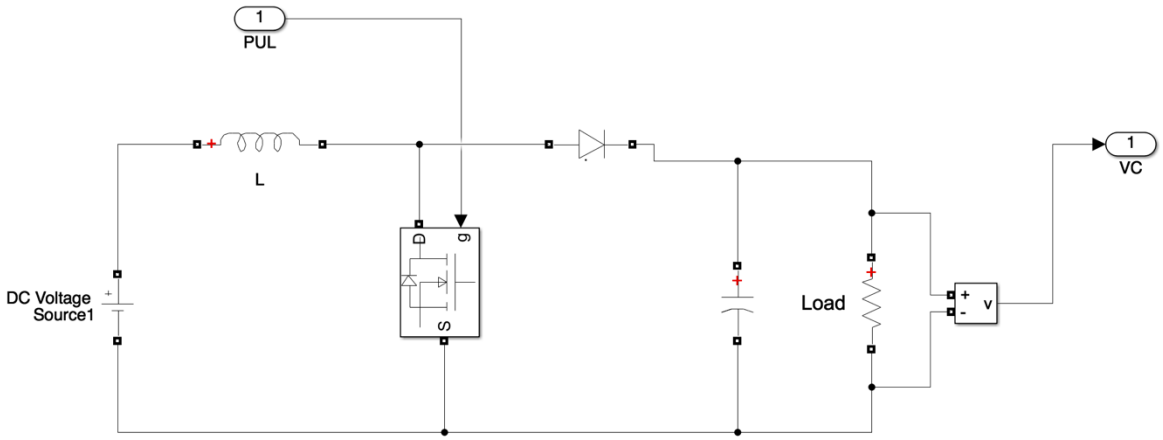

Figure 6-3. Boost converter circuit.

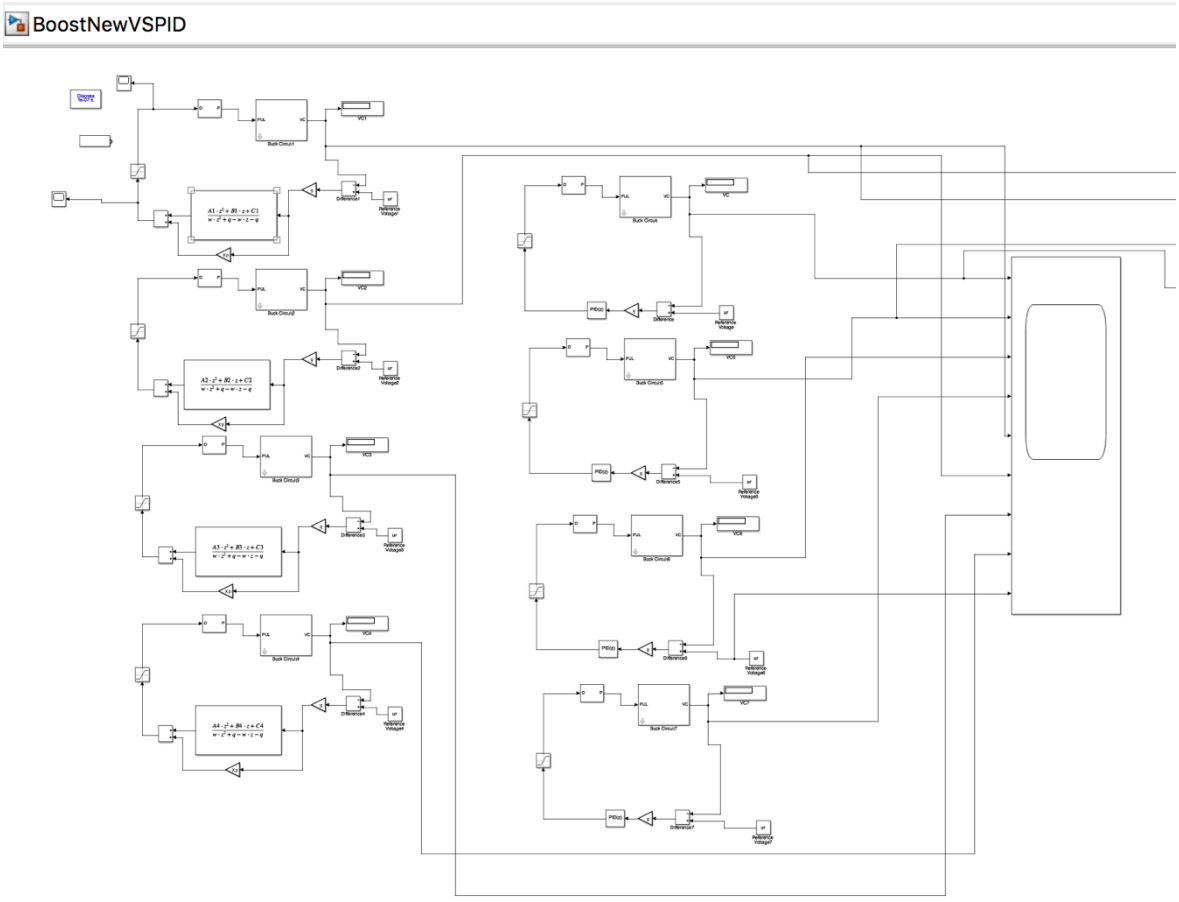

Figure 6-4. New PID VS conventional PID on Boost converter.

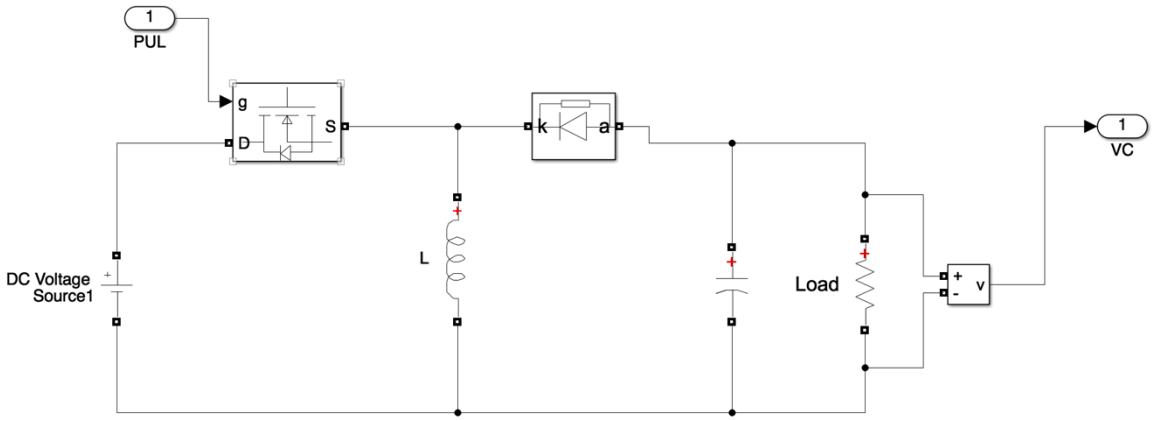

Figure 6-5. Buck-Boost converter circuit.

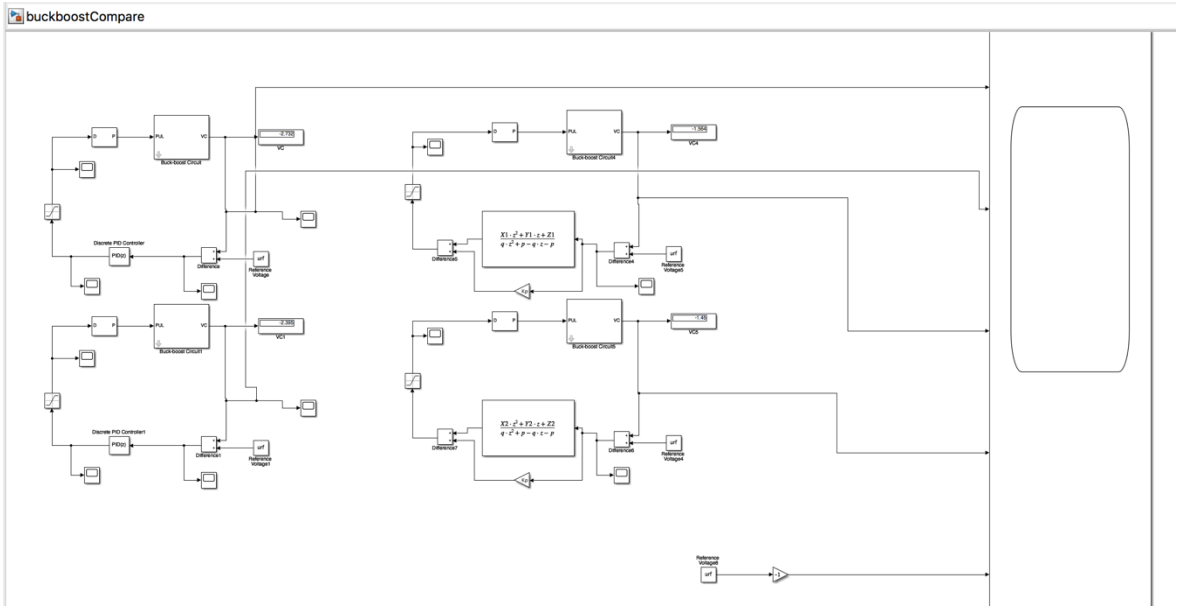

Figure 6-6. New PID VS conventional PID on Buck-Boost converter.